ELSEVIER

Quaternary Science Reviews ▮ (▮▮▮▮) ▮▮▮–▮▮▮

QSR

Holocene thermal maximum in the western Arctic (0–180°W)[☆]

D.S. Kaufman[a,*], T.A. Ager[b], N.J. Anderson[c], P.M. Anderson[d], J.T. Andrews[e], P.J. Bartlein[f], L.B. Brubaker[g], L.L. Coats[h], L.C. Cwynar[i], M.L. Duvall[j], A.S. Dyke[k], M.E. Edwards[l], W.R. Eisner[m], K. Gajewski[n], A. Geirsdóttir[o], F.S. Hu[p], A.E. Jennings[e], M.R. Kaplan[q], M.W. Kerwin[r], A.V. Lozhkin[s], G.M. MacDonald[t], G.H. Miller[e], C.J. Mock[u], W.W. Oswald[d], B.L. Otto-Bliesner[v], D.F. Porinchu[w], K. Rühland[x], J.P. Smol[x], E.J. Steig[d], B.B. Wolfe[y]

[a] *Department of Geology and Environmental Sciences, Northern Arizona University, Flagstaff, AZ 86011-4099, USA*
[b] *US Geological Survey, Denver, CO, USA*
[c] *Geological Survey of Denmark and Greenland, Copenhagen, Denmark*
[d] *Quaternary Research Center, University of Washington, Seattle, USA*
[e] *Institute of Arctic and Alpine Research, University of Colorado, Boulder, USA*
[f] *Department of Geography, University of Oregon, Eugene, USA*
[g] *College of Forest Resources, University of Washington, Seattle, USA*
[h] *Department of Geology, Northern Arizona University, Flagstaff, USA*
[i] *Department of Biology, University of New Brunswick, Fredericton, Canada*
[j] *Department of Geology, Bates College, Lewiston, ME, USA*
[k] *Geological Survey of Canada, Ottawa, Ont., Canada*
[l] *Institute of Geography, University of Trondheim, Norway*
[m] *Department of Geography, University of Cincinnati, Ohio, USA*
[n] *Department of Geography, University of Ottawa, Ontario, Canada*
[o] *Department of Geosciences, University of Iceland, Reykjavik, Iceland*
[p] *Department of Plant Biology, University of Illinois, Urbana, USA*
[q] *School of Geosciences, University of Edinburgh, UK*
[r] *Department of Geography, University of Denver, Colorado, USA*
[s] *Northeast Interdisciplinary Science Research Institute, Russian Academy of Sciences, Magadan, Russia*
[t] *Department of Geography, University of California, Los Angelas, USA*
[u] *Department of Geography, University of South Carolina, Columbia, USA*
[v] *National Center for Atmospheric Research, Boulder, CO, USA*
[w] *Department of Geography, California State University, Long Beach, USA*
[x] *Department of Biology, Queen's University, Kingston, Ont., Canada*
[y] *Department of Geography and Environmental Studies, Wilfrid Laurier University, Waterloo, Ont., Canada*

Received 29 April 2003; accepted 16 September 2003

Abstract

The spatio-temporal pattern of peak Holocene warmth (Holocene thermal maximum, HTM) is traced over 140 sites across the Western Hemisphere of the Arctic (0–180°W; north of ~60°N). Paleoclimate inferences based on a wide variety of proxy indicators

---

[☆] Contribution by PARCS (Paleoenvironmental Arctic Sciences), a research initiative sponsored by the US National Science Foundation. PARCS Holocene Thermal Maximum Working Group members and author affiliations listed in Appendix A.

*Corresponding author. Tel.: +1-435-797-2813; fax: +1-520-523-9220.

E-mail addresses: darrell.kaufman@nau.edu (D.S. Kaufman), tager@usgs.gov (T.A. Ager), nja@geus.dk (N.J. Anderson), pata@u.washington.edu (P.M. Anderson), john.t.andrews@colorado.edu (J.T. Andrews), bartlein@oregon.uoregon.edu (P.J. Bartlein), lbru@u.washington.edu (L.B. Brubaker), larry.coats@nau.edu (L.L. Coats), cwynar@unb.ca (L.C. Cwynar), mduvall@bates.edu (M.L. Duvall), adyke@nrcan.gc.ca (A.S. Dyke), mary.edwards@svt.ntnu.no (M.E. Edwards), wendy.eisner@uc.edu (W.R. Eisner), gajewski@aix1.uottawa.ca (K. Gajewski), age@rhi.hi.is (A. Geirsdóttir), fshu@life.uiuc.edu (F.S. Hu), jenninga@spot.colorado.edu (A.E. Jennings), mkaplan@geo.ed.ac.uk (M.R. Kaplan), mkerwin@du.edu (M.W. Kerwin), lozhkin@neisri.magadan.ru (A.V. Lozhkin), macdonal@geog.ucla.edu (G.M. MacDonald), gmiller@colorado.edu (G.H. Miller), mockcj@gwm.sc.edu (C.J. Mock), woswald@u.washington.edu (W.W. Oswald), ottobli@ncar.ucar.edu (B.L. Otto-Bliesner), porinchu@ucla.edu (D.F. Porinchu), 3kmr5@biology.queensu.ca (K. Rühland), smolj@biology.queensu.ca (J.P. Smol), steig@geophys.washington.edu (E.J. Steig), bwolfe@wlu.ca (B.B. Wolfe).

doi:10.1016/j.quascirev.2003.09.007

provide clear evidence for warmer-than-present conditions at 120 of these sites. At the 16 terrestrial sites where quantitative estimates have been obtained, local HTM temperatures (primarily summer estimates) were on average 1.6±0.8°C higher than present (approximate average of the 20th century), but the warming was time-transgressive across the western Arctic. As the precession-driven summer insolation anomaly peaked 12–10 ka (thousands of calendar years ago), warming was concentrated in northwest North America, while cool conditions lingered in the northeast. Alaska and northwest Canada experienced the HTM between ca. 11 and 9 ka, about 4000 yr prior to the HTM in northeast Canada. The delayed warming in Quebec and Labrador was linked to the residual Laurentide Ice Sheet, which chilled the region through its impact on surface energy balance and ocean circulation. The lingering ice also attests to the inherent asymmetry of atmospheric and oceanic circulation that predisposes the region to glaciation and modulates the pattern of climatic change. The spatial asymmetry of warming during the HTM resembles the pattern of warming observed in the Arctic over the last several decades. Although the two warmings are described at different temporal scales, and the HTM was additionally affected by the residual Laurentide ice, the similarities suggest there might be a preferred mode of variability in the atmospheric circulation that generates a recurrent pattern of warming under positive radiative forcing. Unlike the HTM, however, future warming will not be counterbalanced by the cooling effect of a residual North American ice sheet.

1. Introduction

Temperatures at high latitudes generally peaked during the first half of the present interglaciation, but the warming occurred at different times and to varying degrees in different places. In the Arctic, previous research has shown strong spatial variability in the response to insolation forcing during the early Holocene (CAPE, 2001). This pattern can be examined to understand how climate in the Arctic responded to radiative forcing driven by changes in insolation and other factors. By characterizing the pattern of early Holocene warming, we can hypothesize possible mechanisms that underlie the heterogeneity of the observed response to forcing. Such mechanisms reflect the particular geography of the Arctic and its feedback processes that might influence the pattern and magnitude of potential future changes. The spatial pattern of the Holocene thermal maximum (HTM) can, for example, be compared with the observed pattern of recent warming, and with the characteristic signatures of modes of variability known from the instrumental record.

Spatial variations in the timing and magnitude of circum-Arctic climatic changes have long attracted the attention of researchers. For example, Chamberlin (1899) ascribed the longitudinal asymmetry in the distribution of present and past glaciers around the Arctic to the asymmetry in atmospheric circulation associated with the geographic distribution of continents and oceans. More recent studies have investigated the spatio-temporal pattern of Quaternary climatic change by comparing paleoenvironmental data with numerical climate model output (e.g., COHMAP, 1988; Bartlein et al., 1998; Crucifix et al., 2002). These studies attribute trends in Holocene climate to a range of forcing mechanisms: insolation changes governed by orbital variations, the impact of the Laurentide Ice Sheet in northeast North America on atmospheric circulation and sea-surface temperature (SST), feedbacks from land and ocean cover; atmospheric trace-gas concentrations, and changes in coupled atmospheric–oceanic dynamics, including synoptic-scale circulation features, wind-driven sea-ice dynamics, and the global thermohaline circulation. The local effects of these broader-scale forcings were then modulated by numerous local-scale factors including topography, degree of soil development, and vegetation type (Chapin et al., 2000; Eugster et al., 2000; Keyser et al., 2000; Rupp et al., 2000).

This paper reviews the available data on the timing and spatial pattern of the HTM—the interval of warmth associated with the peak Holocene temperature—in the western Arctic (0–180°W longitude). The review builds upon the framework developed recently by an international effort to synthesize Holocene paleoclimate data for the entire Arctic (CAPE, 2001). Rather than data–model comparisons at key times, however, we focus on the spatio-temporal pattern of a time-transgressive interval when temperatures reached their local HTM.

As used here, the “western Arctic” includes the part of the Arctic within the Western Hemisphere (0–180°W longitude) north of about 60°N latitude (Fig. 1). It extends from Northeast Russia to Iceland, and includes all of the North American Arctic. This Hemisphere encompasses several key features of Arctic geography, oceanography, and climatology. Among these are the Greenland Ice Sheet, the only continental-scale glacier in the Arctic to survive the present interglaciation, the Bering Strait, the principal inflow of marine water from the Pacific to the Arctic Ocean, the Fram Strait, the primary avenue for water exchange between the Arctic Ocean and the global ocean, and the Labrador and Iceland seas, primary sites of North Atlantic Deepwater formation.

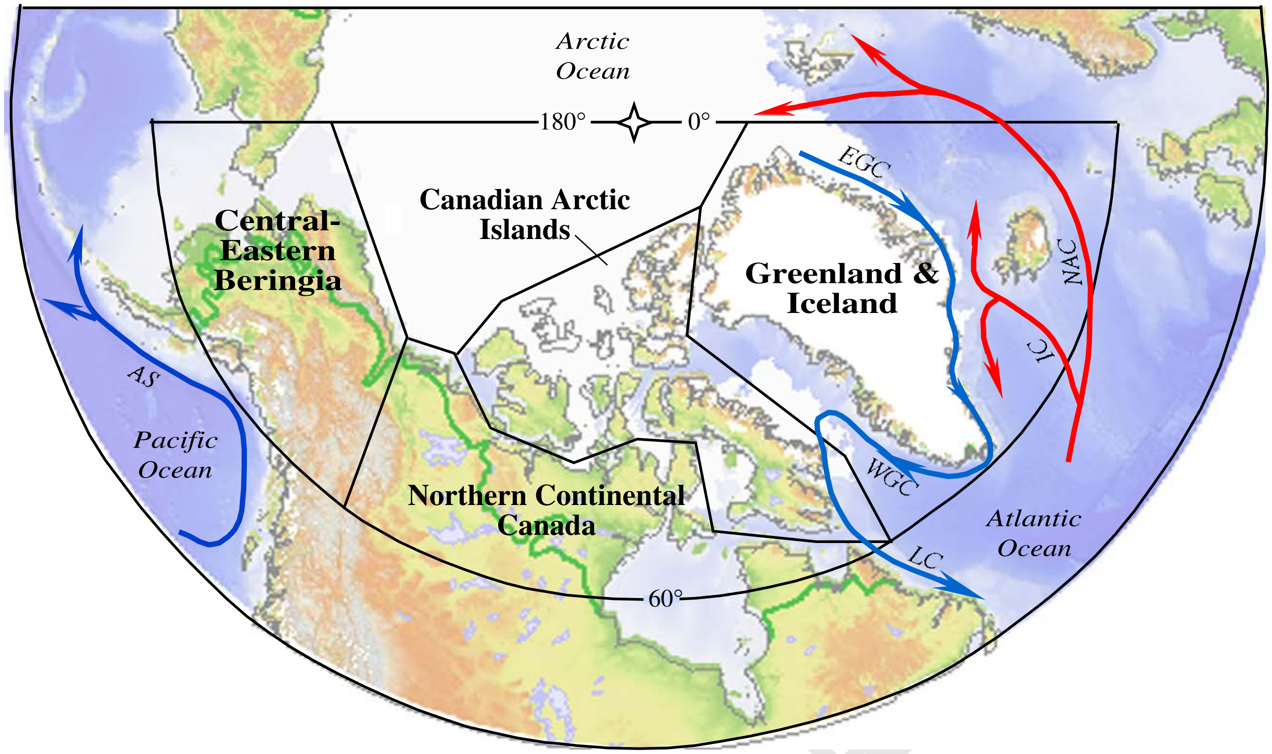

Fig. 1. Western Arctic showing the four major regions reviewed in this paper and generalized ocean surface currents mentioned in text. AS = Alaska Stream; EGC = East Greenland Current; IC = Irminger Current; LC = Labrador Current; NAC = North Atlatic Current; WGC = West Greenland Current. Green line approximates modern treeline. Blue lines mark cold-water currents and red lines are warm Atlantic currents discussed in text.

2. Methods and approach

We compiled an extensive, although not exhaustive, database of unpublished and published records of Holocene paleoenvironmental change from the western Arctic (Table 1; available at: http://www.ngdc.noaa.gov/paleo/parcs/warm_holocene.html) concentrating on continuous records from lakes and marginal seas. The database includes 140 sites (Fig. 2) where organic and inorganic materials from lake and marine sediment, peat deposits, glacier ice, and boreholes have been used for paleoclimatic inferences. Nearly all sites have continuous records of paleoenvironmental change. Most (70%) extend beyond 10 ka; shorter records were included from sites that were ice covered until after 10 ka.

A variety of methods have been used to reconstruct trends in Holocene climate and to determine the timing of the HTM. Each proxy indicator has a characteristic response time and sensitivity to climatic variations, and each responds to different factors of the climate system. Different proxies from the same record can therefore yield different inferences about the timing and magnitude of climatic change. We use multiple proxies wherever they are available because theyprovide the strongest paleoclimatic inferences (Birks and Birks, 1980).

Most of the records in our database rely on pollen and plant macrofossils to infer growing-season temperature of terrestrial vegetation. Because many sites experienced the HTM soon after local deglaciation, it is difficult in some cases to distinguish the direct effects of climate from non-climatic factors, such as deglacial processes and delays related to plant dispersal. Furthermore, lakes differ in their sensitivity to climatic change, and interpretation of proxies can be confounded by processes associated with lake ontongeny, especially for lakes at less extreme, subarctic settings (e.g., Anderson et al., in press). In addition to vegetation changes, other studies included in this review base their paleoclimatic inferences on the assemblage and abundance of fossil organisms in lake and marine sediment, the range of extralimital marine animals, and the temperatures measured in boreholes in ice, among others. Most proxies relate qualitatively to summer temperature, a key climatic variable at high latitude; a small subset of studies has estimated produced quantitative estimates of Holocene temperature. The quantitative estimates are based on microfossil assemblages, treeline position, and stable-isotope composition, each converted to temperature using transfer functions based on modern calibration. Borehole temperatures rely on physical models of thermal diffusivity to reconstruct past mean annual temperature. Inferences based on data derived from

Table 1
Sites used to reconstruct the spatial and temporal pattern of the Holocene thermal maximum in the western Arctic

Site ID[a]	Site name	Lat. (°N)	Long long. (°W)	Initiation (cal ka)[b]	Termination (cal ka)[b]	Citation
Central and eastern Beringia						
1	Elgytgytgyn Lake	67.50	−172.10	No HTM		Shilo et al. (2001)
2	Gytgykai Lake	63.17	−175.00	No HTM		Lozhkin et al. (1998a)
3	Patricia Lake	63.17	−176.75	No HTM		Lozhkin et al. (1995)
4	Jack London Lake	70.83	179.75	11.6	10.6	Lozhkin et al. (2001)
5	Kresta Gulf exposure	66.00	179.00	9.5	8.9	Anderson et al. (2002b)
6	Lorino exposure	65.50	171.70	9.5	8.9	Anderson et al. (2002b)
7	St. Lawrence is Section 3	63.75	171.50	10.5	9.0	Lozhkin et al. (1998b)
8	Flora Lake	63.30	170.30	No HTM		Colinvaux (1967a)
9	North Killeak Lake	66.33	164.17	13.0	12.4	P.M. Anderson, unpub. data
10	Tungak Lake	61.23	164.01	No HTM		Ager (1982)
11	Zagoskin Lake	63.45	162.11	13.1	11.6	Ager (1983, 2003)
12	Squirrel Lake	67.10	160.38	14.2	12.0	P.M. Anderson, unpub. data
13	Niliq Lake	67.52	159.73	12.9	12.5	Anderson (1988)
14	Ongivinuk Lake	59.57	159.37	No HTM		Hu et al. (1996)
15	Grandfather Lake	59.80	158.52	No HTM		Hu et al. (1996)
16	Meade River	70.47	157.47	10.8	8.5	Eisner and Peterson (1998)
17	Joe Lake	66.47	156.87	12.6	11.3	Anderson (1988)
18	Etivlik Lake	68.08	155.98	No HTM		P.M. Anderson, unpub. data
19	Idavain Lake	58.77	155.95	10.0	9.4	Brubaker et al. (2001)
20	Headwaters Lake	67.93	155.05	No HTM		Brubaker et al. (1983)
21	Snipe Lake	60.64	154.28	No HTM		Patricia Anderson, unpub. data
22	Angal Lake	67.13	153.90	13.3	11.4	Brubaker et al. (1983)
23	Ranger Lake	67.15	153.65	No HTM		Brubaker et al. (1983)
24	Farewell Lake	62.55	153.63	9.7	9.1	Hu et al. (1998)
25	Redstone Lake	67.15	151.63	No HTM		Edwards et al. (1985)
26	Screaming Yellowlegs Pond	67.58	151.42	12.3	10.5	Edwards et al. (1985
27	Rebel Lake	67.42	149.80	No HTM		Edwards et al. (1985)
28	Imnavait Creek	68.67	149.33	13.0	9.8	Eisner (1991)
29	Crowsnest Lake	68.33	146.48	No HTM		P.M. Anderson, unpub. data
30	Honeymoon Pond	64.62	138.40	10.5	7.4	Cwynar and Spear (1995)
31	Sulpher Lake	60.95	137.95	8.8	6.9	Lacourse and Gajewski (2000)
32	Lake U60 (stinky lake)	62.75	136.63	12.5	8.8	Pienitz et al. (2000)
33	Lateral Pond	65.95	135.93	No HTM		Ritchie and Cwynar (1982)
34	Sleet Lake	69.29	133.82	11.6	7.7	Spear (1993); Ritchie et al. (1983)
35	Kettlehole Pond	60.06	133.80	10.1	7.0	Cwynar and Spear (1995)
36	Twin Tamarack Lake	68.30	133.42	12.9	7.9	Ritchie et al. (1983); Spear (1983)
37	Tuktoyuktuk 5	69.10	133.40	9.7	6.1	Ritchie and Hare (1971)
38	Campbell Creek Peatland	69.28	133.25	9.5	6.3	Vardy et al. (1998)
39	Reindeer Lake	69.17	132.32	9.6	7.7	Spear (1993)
40	Sweet Little Lake	67.65	132.02	11.6	8.0	G.M. MacDonald, unpub. data
41	Bluffers Pingo	69.74	131.89	11.6	8.0	Spear (1993)
42	Candelabra Lake	61.68	130.65	10.9	7.4	Cwynar and Spear (1995)
Northern continental Canada						
43	Natla Bog	63.02	128.80	9.1	5.6	MacDonald (1983)
44	Andy Lake	64.65	128.08	10.0	7.0	Szeicz et al. (1995)
45	Keele Lake	64.17	127.62	9.0	7.0	Szeicz et al. (1995)
46	Bell's Lake	65.02	127.43	9.0	7.0	Szeicz et al. (1995)
47	Lac Meleze	65.22	126.12	No HTM		MacDonald (1987)
48	Hail Lake	60.03	126.02	10.1	6.9	Cwynar and Spear (1995)
49	Lake BC2	58.46	124.46	10.6	7.5	Pisaric et al. (2003)
54	Lac Demain	62.05	118.70	No HTM		MacDonald (1987)
56	Wild Spear Lake	59.25	114.15	No HTM		MacDonald (1987)
58	McMaster Lake	64.10	110.57	5.6	4.4	MacDonald et al. (1993) and Moser and MacDonald (1990)
59	Queens Lake	64.12	110.57	5.6	4.4	MacDonald et al. (1993), Moser and MacDonald (1990) and Edwards et al. (1996)
60	Toronto Lake	63.71	109.35	6.9	3.2	MacDonald et al. (1993) and Moser and MacDonald (1990)

Table 1 (*continued*)

Site ID^{a}	Site name	Lat. (°N)	Long long. (°W)	Initiation (cal ka)^{b}	Termination (cal ka)^{b}	Citation
61	Waterloo Lake	63.73	108.10	6.9	3.2	MacDonald et al. (1993) and Moser and MacDonald (1990)
62	Lake TK-20	64.09	107.49	7.1	3.6	Rühland (2001)
70	Lake BI2	57.12	76.38	6.6	0.8	Gajewski and Garralla (1992)
71	Lake LB1	57.92	75.62	6.7	1.1	Gajewski et al. (1993)
72	Lake GB2	56.10	75.28	6.7	0.8	Gajewski et al. (1993)
73	Lake LR1	58.58	75.25	6.0	4.4	Gajewski et al. (1993)
74	Lake LR3	58.50	75.25	6.3	5.0	Gajewski and Garralla (1992)
75	Lake LT1	59.15	75.15	6.0	5.6	Gajewski and Garralla (1992)
78	Lake RAF1	58.23	72.07	5.0	2.0	Richard (1981)
80	Diana 375 Lake	60.99	69.96	7.0	5.4	Richard (1981) and Kerwin et al. (submitted)
89	Ublik Pond	57.38	62.05	7.8	2.6	Short and Nichols (1977) and Kerwin et al. (submitted)
90	Nain Pond	56.53	61.82	6.3	1.0	Short and Nichols (1977) and Kerwin et al. (submitted)
94	HU87033-017 and HU87033-018	54.61	56.17	6.8	5.5	Andrews et al. (1999)
Canadian Arctic Islands						
50	74MS11	71.75	124.27	7.9	2.1	Gajewski et al. (2000)
51	Muskox Lake	71.78	122.67	7.9	2.1	Gajewski et al. (2000)
52	74MS15	73.53	120.22	7.9	2.1	Gajewski et al. (2000)
53	74MS12	72.37	119.83	7.9	2.1	Gajewski et al. (2000)
55	Beaufort Sea bowheads^{c}	70.10	116.60	11.5	9.5	PARCS website
57	Western archipelago molluscs^{c}	69.40	114.00	11.5	8.5	PARCS website
63	Lake PWWL	73.57	98.48	7.5	4.0	Gajewski and Frappier (2001)
64	Lake RS29	73.13	95.28	10.0	5.0	Gajewski (1995)
65	Lake RS36	72.58	95.07	11.0	6.0	Gajewski (1995)
66	Central archipelago bowheads^{c}	72.64	94.16	11.0	9.0	PARCS website
67	Eastern archipelago bowheads^{c}	75.20	86.90	11.0	8.5	PARCS website
68	N Baffin Island bowheadsc	71.90	85.00	5.5	2.5	PARCS website
69	Rock Basin Lake	78.50	76.79	7.8	4.5	Smol (1983) and Hyvärinen (1985)
76	91039	77.27	74.33	8.8	4.5	Levac et al. (2001)
77	Agassiz Ice Cap	80.70	73.10	9.5	6.8	Koerner and Fisher (1990), Fisher et al. (1995) and Fisher and Koerner (2003)
79	NE Baffin Island molluscs^{c}	70.06	71.60	9.5	7.5	PARCS website
81	Patricia Bay Lake	70.47	68.50	7.5	5.8	Mode (1980)
82	Lake Hazen region	82.88	68.43	5.5	2.0	Smith (2002)
83	Hikwa Lake	63.30	67.36	4.9	2.1	Mode and Jacobs (1987)
84	INQUA Lake	62.27	66.23	7.4	4.5	Miller, unpub. data
85	Amarok Lake	66.28	65.75	10.2	9.3	Wolfe (1994, 1996)
86	Penny Ice Cap	67.00	65.50	9.5	6.8	Fisher et al. (1998)
87	Robinson Lake	63.40	64.27	7.8	4.5	Miller et al. (1999)
88	Fog Lake	67.18	63.25	7.6	4.2	Wolfe et al. (2000)
91	Donard Lake	66.66	61.78	7.6	1.0	S.K. Short, unpub. data; Kerwin et al. (submitted)
92	Dyer Lower Lake	66.62	61.65	7.6	2.6	S.K. Short, unpub. data; Kerwin et al. (submitted)
Greenland and Iceland, terrestrial sites						
93	Camp Century	77.18	61.12	8.0	4.1	Dansgaard et al. (1971)
96	Lake NAUG1	66.48	52.18	No HTM		Willemse and Törnqvist (1999)
97	Tetra Lake A	64.47	51.58	6.0	2.5	Fredskild (1983)
98	Lake SS6	66.98	51.11	7.0	4.0	McGowan et al. (2003)
99	Braya Sø	66.99	51.05	7.0	4.0	McGowan et al. (2003)
100	Lake SS2	66.98	50.97	No HTM		N.J. Anderson, unpub. data
101	St Salt Sø	66.98	50.58	7.0	6.5	Bennike (2000)
102	Lake 31	67.05	50.47	4.9	3.7	Eisner et al. (1995)

Table 1 (*continued*)

Site ID[a]	Site name	Lat. (°N)	Long long. (°W)	Initiation (cal ka)[b]	Termination (cal ka)[b]	Citation
103	Johs Iversen	64.40	50.20	6.2	4.0	Fredskild (1983)
104	Qipisarqo Lake	61.01	47.75	6.6	2.1	Kaplan et al. (2002)
105	Dye 3	65.20	43.8	6.0	3.0	Dahl-Jensen et al. (1998)
106	North GRIP	75.02	41.20	8.6	4.3	Johnsen et al. (2001)
107	GISP2	72.60	38.50	8.2	6.5	Grootes et al. (1993)
108	GISP2	72.60	38.50	8.2	6.5	Cuffey and Clow (1997)
109	GRIP	72.60	37.60	8.2	6.0	Johnsen et al. (2001)
110	GRIP	72.60	37.60	8.2	4.5	Dahl-Jensen et al. (1998)
116	Renland	71.30	26.73	8.5	5.5	Johnsen et al. (1992)
118	Lake N1, Ymer Ø	73.33	25.20	7.7	5.0	Wagner and Melles (2002)
120	Efstadalsvatn, Laugardalur	65.93	22.66	9.1	6.8	Caseldine et al. (2003)
121	Lake Basaltsø	72.72	22.47	9.0	6.5	Wagner et al. (2000) and Cremer et al. (2001a)
122	Raffles Ø Lake	70.58	21.90	7.5	4.0	Wagner and Melles (2001) and Cremer et al. (2001b)
125	Zackenberg delta	74.50	20.50	9.5	6.3	Christiansen et al. (2002)
126	Lómatjörn	64.26	20.35	9.1	5.6	Vasari and Vasari (1990)
127	Hafratjörn	65.58	20.13	9.8	5.7	Vasari and Vasari (1990)
128	Nioghalvfjerdsfjorden	79.83	19.65	7.7	4.5	Bennike and Weidick (2001)
129	Vatnskotsvatn	65.70	19.48	9.7	5.6	Hallsdóttir (1995)
131	Vesturardalur 2	65.75	18.72	8.6	6.7	Wastl et al. (2001)
133	Krosshoosmyri, Flateyjardalur	66.08	17.90	10.3	5.6	Hallsdóttir (1991)
Greenland and Iceland, marine sites						
95	West Greenland molluscs[c]	67.24	52.50	10.5	6.0	PARCS website
111	JM96-1214/2-GC	67.30	30.97	9.8	7.0	Smith (2001)
112	JM96-1216/1-GC	65.96	30.63	9.0	7.2	Hagen (1995)
113	BS1191-K15	68.10	29.45	9.0	5.0	Andrews et al. (1997)
114	JM96-1207/2-GC (1206/1-GC)	68.10	29.35	6.5	4.0	Jennings et al. (2002)
115	JM96-1205/2-GC	68.07	27.84	8.0	4.0	Smith (2001)
117	MD952015	58.76	25.95	10.6	6.0	Giraudeau et al. (2000)
119	East Greenland molluscs[c]	72.08	24.30	10.5	6.0	PARCS website
123	B997-330	65.87	21.08	8.0	7.0	Andrews and Giraudeau (2003)
124	MD99-2269	66.62	20.85	9.0	4.9	Andrews et al. (2002); N. Koç unpub. data
130	HM107-04	67.22	19.05	10.7	6.1	Eirîksson et al. (2000)
132	HM107-05	66.90	17.90	10.3	7.0	Eirîksson et al. (2000)
134	PS21842-5	69.46	16.51	9.6	7.9	Koç et al. (1993)
135	HM57-5	69.43	13.11	10.4	6.0	Koç et al. (1993)
136	MD95-2011	66.96	7.60	9.0	6.7	Birks and Koç (2002)
137	HM57-14	67.00	6.20	10.6	9.0	Koç et al. (1993)
138	HM79-26	66.90	5.93	10.6	4.1	Koç et al. (1993)
139	HM79-6.2(6/4)	62.96	2.70	11.1	5.7	Birks and Koç (2002), Karpuz and Jansen (1992) and N. Koç unpub. Data
140	HM94-13	71.62	1.62	7.9	5.6	Koç et al. (1993)

[a] Sites arranged by longitude within each of the four regions (Fig. 2). Site IDs keyed to PARCS on-line database (http://www.ngdc.noaa.gov/paleo/parcs/.html), where additional information is tabulated on the availability of raw data in electronic format, site location, proxy indicator, quality of age control, and rationale of paleoclimatic inferences.

[b] Initiation and terminations refer to the timing of the onset and ending of the Holocene thermal maximum (HTM). ND = HTM was not detected by the paleoclimatic proxy evidence.

[c] Locations for bowhead whale and mollusc records are the average latitude and longitude of many ^{14}C sample collection sites, subdivided into groups on the basis of geographic clusters. Ages were tabulated and frequency distributions derived using a bin size of 500 yr.

transfer functions generally rely on a comparison with modern conditions as indicated by the uppermost samples in a stratigraphic record, which typically integrate the 20th century. Only a few studies have reconstructed effective moisture using stable isotopes and sedimentological evidence of lake-level changes or snow accumulation rates.

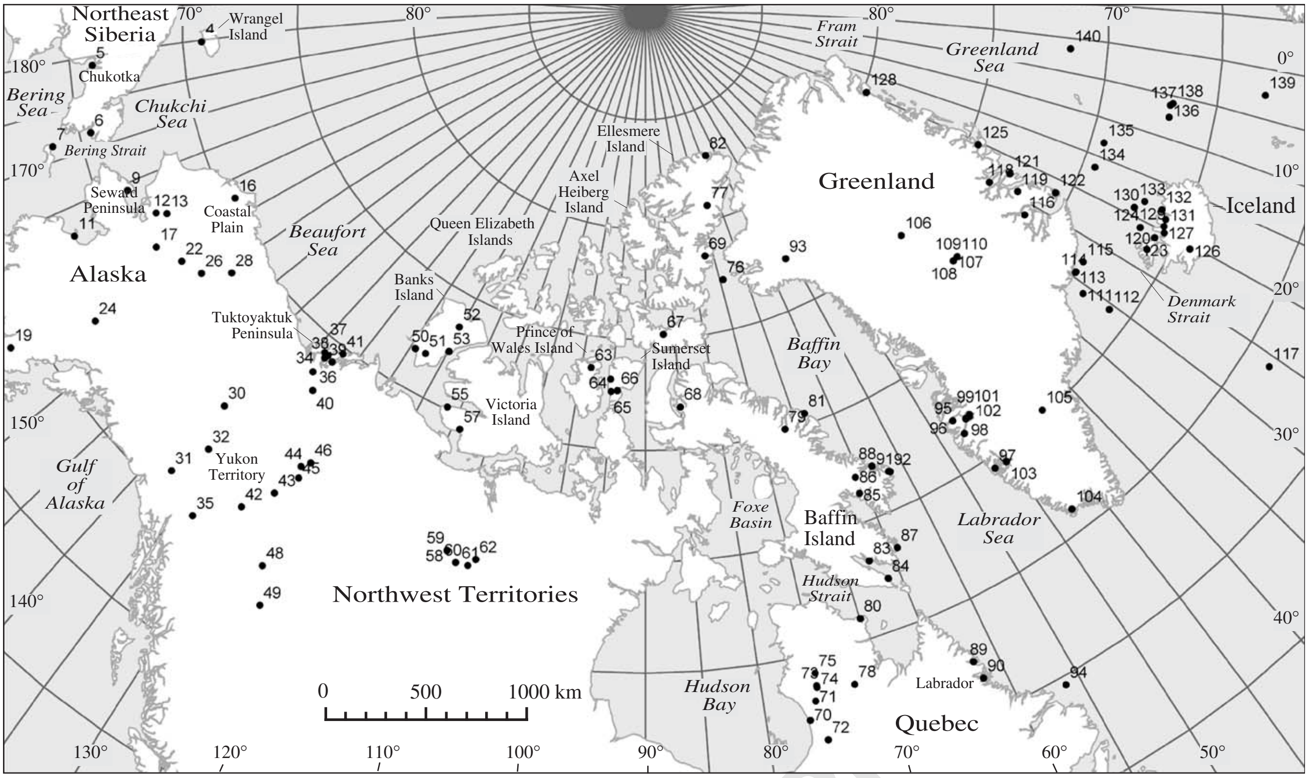

Fig. 2. Western Arctic showing geographic features mentioned in text and locations of sites where evidence of the HTM has been studied. Site numbers arranged by longitude and are keyed to Table 1.

Uncertainties in reconstructing the spatio-temporal pattern of the HTM stem from problems associated with chronological control. Nearly all records in the database have timescales based on ^{14}C (ice cores are a notable exception). The accuracy of the age models varies among sites, and is related to a variety of factors involving the type of material that is analyzed (e.g., bulk sediment or macrofossils), the origin of its carbon, and sediment reworking, among others. Accurately dating sediment from lakes with a paucity of macrofossils, common at high latitudes, is particularly difficult. Studies that were based on fewer than three ^{14}C analyses for the Holocene were excluded. The age models for the lake- and marine-sediment records in our database are supported by an average of one ^{14}C date per 2500 yr. Errors in age models are undoubtedly the source of some of the apparent spatial variability, especially at centennial timescales. Rather than screening individual records that appear suspect, we retained the widest data set and focus on the most robust trends that are clearly exhibited at the millennial scale.

In some cases, the authors of previously published studies explicitly stated the timing of the HTM, and the original interpretation is usually retained in this paper, or, in some cases, modified by the author for this study. In other cases, the timing of the HTM was interpreted by Working Group authors responsible for the regional summaries. For example, we tabulated new and previously published ^{14}C ages on extralimital mollusk shells and whale bones from the Canadian Arctic Islands and East Greenland, and derived frequency histograms for select regions to infer the timing of maximum warmth. A listing of these ages and their sample locations, along with the sources and rationale of the paleoclimatic inferences for all sites, and the location of the original data, are provided in the HTM database at the PARCS website.

Rarely is the age of the HTM constrained by ^{14}C ages directly adjacent to the boundaries of this interval. Therefore, authors' original age models were used to interpolate the age of the HTM in ^{14}C years. Ages were then calibrated without estimating an associated analytical error. Calibrated ages are either the mid-point of the 1σ range from the output of CALIB (Stuiver and Reiner, 1993), or derived for the purposes of this study from a third-order polynomial fit to the CALIB data (cal age $= 10^{-9}C^3 - 10^{-5}C^2 + 1.2C - 210$, where $C = {}^{14}$C age in yr BP). The average difference between the mid-point of the 1σ range and the polynomial fit is about 150 yr for the time interval of interest. Some ages were based on age models that were calibrated by the original authors. Although the specific method of calibration differs among authors, the associated error is probably much smaller than the accuracy of the age models themselves, and is negligible in comparison to the subjectivity in choosing the age boundaries (initiation and termination) of the HTM, which were chosen to bracket the interval of maximum post-glacial warmth. All ages given in this paper are in calendar years.

3. Spatio-temporal pattern of the Holocene thermal maximum

We subdivide the western Arctic into four major regions, each with distinctive geographic and oceanographic settings and unique antecedent conditions leading into the HTM. They are from southwest to northeast: central and eastern Beringia, northern continental Canada, Canadian Arctic Islands, and Greenland and Iceland (Fig. 1).

3.1. Central and eastern Beringia

3.1.1. Physiographic and antecedent conditions

This region extends from Northeast Russia east to the Mackenzie River. As a whole, Beringia includes all of eastern Siberia, but because this review focuses on the Western Hemisphere, we discuss only central and eastern Beringia. Differences are evident among three subregions: (1) central Beringia, which includes Northeast Russia, the epicontinental Bering and Chukchi seas, and westernmost Alaska; (2) Alaska; and (3) Canadian Beringia. The region is bordered on the south by the North Pacific Ocean, with its prevailing easterly surface currents (the Alaska Stream) that branch northward through Bering Strait; on the north is the Beaufort Sea, with surface currents dominated by the southern limb of the Arctic Ocean gyre.

Two physiographic features of the region strongly influenced the evolution of its climate during the Holocene: the vastness of its unglaciated area, and the breadth of its shallow continental shelves. Most of Beringia remained ice-free during the last glacial maximum. As summer insolation increased during the early Holocene, this was the largest region in the western Arctic where solar energy was absorbed by land rather than reflected by ice. While this must have facilitated a relatively rapid response to insolation forcing, the resultant warming was tempered by the concurrent flooding of the epicontinental shelves. As eustatic sea level rose, the Beringian continent was severed by coastlines that transgressed >700 km northward from the Pacific Ocean and southward from the Arctic Ocean. Nearly $2\times10^6\,\mathrm{km}^2$ of emerged shelf was flooded following the last glacial maximum, transforming central Beringia from a continental interior to a coastal maritime environment. The shoreline transgressed most rapidly as summer insolation peaked, which probably moderated the effects of increasing summer insolation and increased the moisture content of the troposphere over eastern Beringia.

3.1.2. Central Beringia

Paleoclimatic inferences for central Beringia are drawn primarily from pollen records, which are sparse and have varying levels of chronological control (Anderson et al., 2002a). The only continuous Holocene lake records available from mainland areas of eastern Chukotka (Elgytgytgyn, Gytgykai, and Patricia lakes; Table 1 sites 1–3) indicate gradual post-glacial warming beginning ca. 14.9 ka and continuing through the early Holocene, with no indication of an HTM prior to the mid-Holocene. This interpretation is based on trends in *Pinus pumila* pollen (Fig. 3a). Of all shrubs represented in the Chukotkan Holocene records, *P. pumila* requires the greatest summer warmth (mean July temperature of 12°C; Kozhevnikov, 1981). In contrast, buried organic-rich deposits at two near-coastal sites in Chukotka (Lorino and Kresta Gulf exposures; sites 5 and 6) suggest climates may have been slightly warmer than present between ca. 9.7 and 9.2 ka. The strongest evidence for the HTM in eastern Chukotka comes from its northernmost sites. Peat began to accumulate on Wrangel Island ca. 12.9 ka and continued through the early Holocene (Vartanyan, 1997; Lozhkin et al., 2001) whereas organic deposits do not accumulate on the island today, suggesting conditions were warmer and wetter than present, with modern vegetation established as recently as 4.4–3.3 ka (Vartanyan, 1997).

Holocene records from the Bering Sea region, spanning from the Aleutians northward to St. Lawrence Island, are dominated by herb taxa, indicating the presence of tundra throughout the Holocene. Initial studies on St. Lawrence Island (site 8) did not document significant palynological variations during the Holocene, and indications of the HTM are absent from the Pribilof Islands (S Bering Sea; Colinvaux, 1967b, 1981). However, more recent work on peat deposits (site 7) suggests warmer-than-present conditions began ca. 10.5 ka, perhaps terminating near 9 ka. Tungak Lake (SW Alaska; site 10), the most southerly mainland record in central Beringia, shows no indication of an HTM, whereas two lakes farther north show a westward expansion of *Populus* beyond its modern limit. At Zagoskin Lake (W Alaska, site 11), *Populus* forest was established ca. 13.1–11.6 ka, and replaced by shrub tundra during the early Holocene. At North Killeak Lake (N Seward Peninsula; site 9), pollen data suggest *Populus* woodland was present sometime after ca. 13 ka.

3.1.3. Alaska

Various proxies imply an interval of warmer-than-present temperatures between 11.5 and 9 ka in Alaska. Biological evidence includes the latitudinal range extension of several animal and plant taxa. For example, beetles found beyond their modern limits on the Arctic Coastal Plain indicate summer temperatures of +2–3°C ca. 10.8 ka (Nelson and Carter, 1987), and beaver-

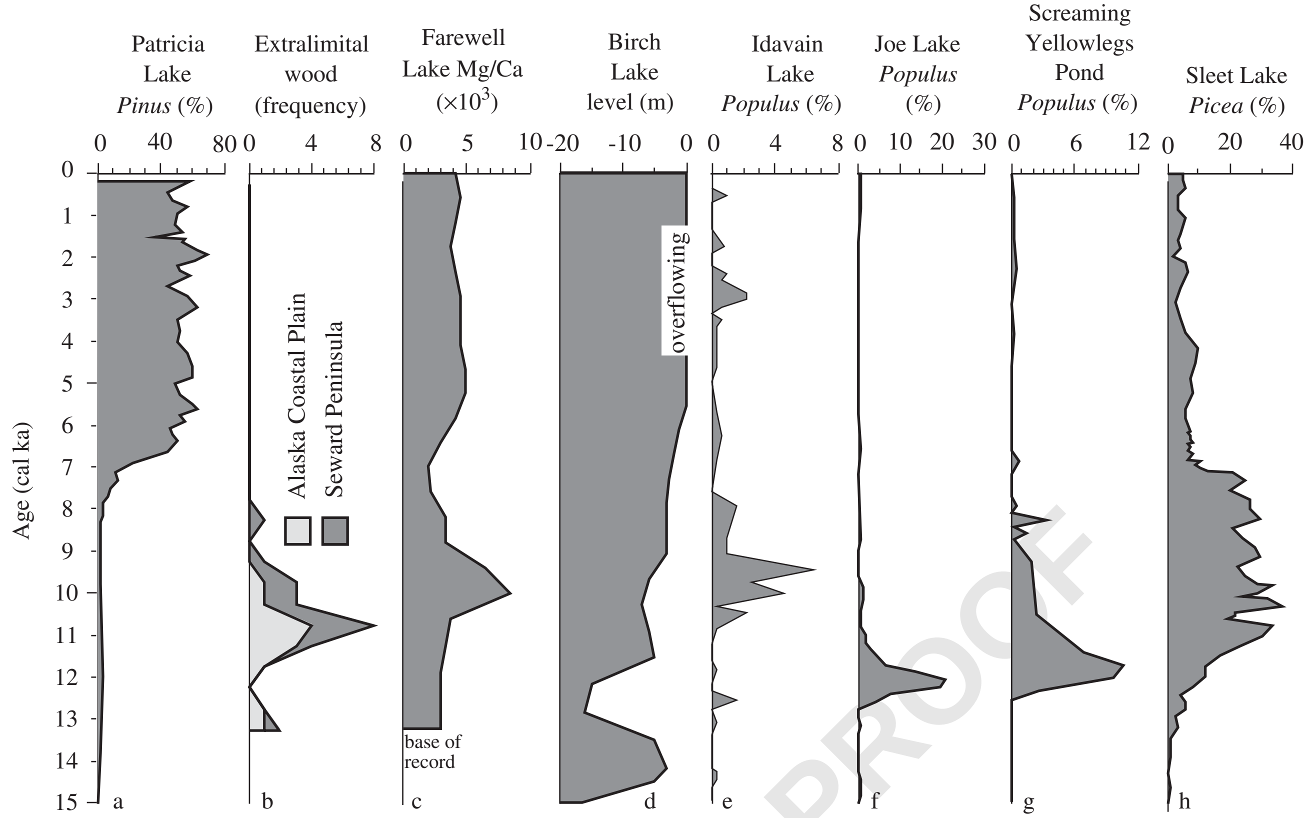

Fig. 3. Selected records of the HTM from central and eastern Beringia, arranged roughly from west to east. (a) *Pinus* subg. *strobus* pollen percentage, Patricia Lake, northeast Siberia (Lozhkin et al., 1995); the rise in *Pinus* following 7 ka represents the establishment of modern vegetation without evidence for warmer-than-present conditions anytime during the Holocene; this record contrasts with one from Wrangel Island, where warming took place between 11 and 9 ka (Vartanyan, 1997). (b) Number of ^{14}C ages on *Populus* wood beyond the range of trees on Seward Peninsula and the North Slope; Seward Peninsula ages include beaver-gnawed wood, not necessarily *Populus*, but beyond the modern range of beaver; bin size = 500 yr (compiled from Hopkins et al., 1981; Kaufman and Hopkins, 1985; Mann et al., 2002). (c) Mg/Ca molar ratios in ostracode shells. Farewell Lake, northwest Alaska Range (Hu et al., 1998). (d) Lake-level changes, Birch Lake, interior Alaska (Abbott et al., 2000). (e) *Populus* pollen percentage, Idavain Lake, southwest Alaska (Brubaker et al., 2001). (f) *Populus* pollen percentage, Joe Lake, Brooks Range, Alaska (Anderson, 1988). (g) *Populus* pollen percentage, Screaming Yellowlegs Pond, Brooks Range, Alaska (Edwards et al., 1985). (h) *Picea* pollen percentage from Sleet Lake, northwest Yukon Territory (Ritchie et al., 1983).

gnawed wood on the Seward Peninsula indicates a range extension of beaver ca. 10.5–9.5 ka (McCulloch and Hopkins, 1966; Fig. 3b). Likewise, pollen in lake sediments from northwest Alaska suggests that some aquatic plants expanded beyond their modern ranges (Anderson, 1988), and pollen and macrofossil evidence from many sites in Alaska indicates that *Populus balsamifera* was abundant beyond modern treeline during this interval (Hopkins et al., 1981; Brubaker et al., 1983; Edwards et al., 1985; Anderson, 1988; Mann et al., 2002; Ager, 2003). Dendrochronological analyses demonstrate that *P. balsamifera* responds positively to warm temperatures during early summer (Edwards and Dunwiddie, 1985; Lev, 1987) suggesting conditions warmer than present (although substrate and soil changes also play a role; Hu et al., 1993; Mann et al., 2002).

To emphasize range extensions as evidence for the HTM in Alaska, we focus on sites at or beyond modern treeline. Although evidence of the HTM is absent in many records, relatively high percentages (>2%) of *Populus* pollen occur sometime between 14.2 and 9.4 ka at several sites across northern and western Alaska. Sites within the modern boreal forest offer palynological evidence of compositional changes roughly coincident with the range extensions of *Populus* and other taxa (e.g., Hu et al., 1993; Bigelow and Edwards, 2001), and pollen records from south-central Alaska suggest that the HTM took place between 11.6 and 10.3 ka, when *Alnus sinuata* spread rapidly across the south coastal mountains (Ager, 1983, 1989). The Holocene history of temperature and precipitation changes for the northwest coast of North America, including the Gulf of Alaska region, was reconstructed using pollen-based transfer functions (Heusser et al., 1985; Mann et al., 1998). The reconstruction indicates warmer-than-present conditions from 11 to 10 ka, followed by an interval of nearly

2°C additional warming between 10 and 8 ka, after which temperatures declined steadily until about 5 ka.

Geomorphic evidence for the HTM in Alaska is broadly consistent with the biological proxies. In particular, thaw lakes developed between 12 and 9 ka on the Arctic Coastal Plain (Edwards and Brigham-Grette, 1990), concurrent with the rapid accumulation of peat (Eisner 1991; Eisner and Peterson 1998), ice wedges thawed between 11.6 and 6.5 ka on Seward Peninsula (Hopkins et al., 1960; Hopkins, 1972), and well-developed soils formed ca. 11 ka in the Yukon-Tanana upland (east-central Alaska; Weber et al., 1981; Porter, 1988). Glaciers in the central Brooks Range (N Alaska) retreated behind their modern limits, or perhaps were ablated entirely during the early Holocene (Calkin, 1988), glaciers in the north-central Alaska Range (central Alaska) were less extensive than today sometime between 11 and 7 ka (TenBrink and Waythomas, 1985), and glacier ice disappeared between 9.1 and 3.2 ka in the Ahklun Mountains (SW Alaska; Levy et al., 2003). Along the southern coast of Alaska, glacier termini may have retreated inland from their present positions during the early Holocene (Shephard, 1995; Crossen et al., 2002).

Lake-sediment geochemistry and sedimentary evidence of water-level fluctuations also attests to Holocene climatic variability, but such data are available for only a few sites in Alaska. For example, trace-element analysis of ostracode shells from Farewell Lake (NW Alaska Range, site 24) suggests that temperatures peaked between 9.7 and 9.1 ka (Fig. 3c). Lake-level reconstructions at sites in interior Alaska, including Birch Lake (Fig. 3d) suggest that the early Holocene was warm and dry, with summer precipitation 25–40% lower than today. A subsequent lake-level rise between 10.3 and 9.1 ka indicates an increase in effective moisture (Abbott et al., 2000; Barber and Finney, 2000; Bigelow and Edwards, 2001).

The HTM appears to have been asynchronous across Alaska. Proxies from southwest Alaska, including the pollen record from Idavain Lake (site 19; Fig. 3e), indicate that the HTM occurred sometime between ca. 11 and 7 ka, earlier than in western and northern Alaska. This geographic asynchrony may have resulted from spatially uneven effects of the shoreline transgression over Bering Land Bridge or from synoptic-scale circulation patterns (Edwards et al., 2001); however, dating problems cannot be excluded. Early chronologies based on bulk lake-sediment samples may be too old by 1000–2000 yr (Oswald et al., 1999; Bigelow and Edwards, 2001). Thus, it is likely that the *P. balsamifera* range extension at northern Alaskan sites such as Joe Lake (site 17) and Screaming Yellowlegs Pond (site 26) occurred after ca. 11.5 ka, following the Younger Dryas (Figs. 2f and g).

Overall, evidence of the HTM in Alaska is less striking than in other regions of the western Arctic, and less pronounced than simulated by general circulation models (Bartlein et al., 1998). For example, the *Picea* treeline is not known to have been any farther north during the Holocene than at present, as it was in the Yukon and north-central Canada (Ritchie et al., 1983), although the Brooks Range may have inhibited northward movement. In addition, the timing of the HTM is not well constrained in this region, and the behavior of the paleoclimatic proxies may in some cases be related to factors other than climate. Nevertheless, when considered together the range extensions and other indicators provide reasonable evidence for higher-than-present summer temperatures during the early Holocene.

3.1.4. Yukon Territory and westernmost Mackenzie District

In northwest Canada, summer temperatures were warmer than present beginning 10.6 ka, with a transition to near-modern temperatures between 6.7 and 5.6 ka. The clearest evidence for the HTM is from the Tuktoyaktuk Peninsula, where the forest advanced northward of its present-day limit, and then retreated (Ritchie and Hare, 1971; Spear, 1983, 1993; Ritchie, 1984). High *Picea* pollen values and *Picea* needles in the sediments of Sleet Lake (site 34; Fig. 3h) indicate the presence of forest 75 km north of the modern treeline between 12.2 and 5.6 ka, with peak pollen influx at 10.3 ka. Farther east on the Tuktoyaktuk Peninsula, *Picea* appears to have arrived later, peaking between 10.3 and 9.1 ka (Spear, 1993), and spruce stumps dating to the first half of the Holocene have been found on the tundra of the Tuktoyaktuk Peninsula (Ritchie and Hare, 1971; Spear, 1983; Ritchie, 1984). Range extensions and dendroclimatological evidence suggest that temperature on the Tuktoyaktuk Peninsula was as much as +3°C (Ritchie, 1984). Several taxa, such as *Myrica*, *Typha*, and *Populus*, expanded north of their present ranges in northwest Canada between 11.6 and 5.6 ka and centered on 10.3 ka (Cwynar, 1982; Ritchie et al., 1983). In the alpine tundra of central Yukon, pollen and plant macrofossil evidence from three sites indicates that forest occupied the region from 11.6 to 5.6 ka (Cwynar and Spear, 1991). In the southern Yukon, the pollen evidence is inconclusive as to age of the HTM, but temperatures there (Cwynar, 1988), as in the Yukon in general (Cwynar and Spear, 1995), began to cool toward modern between 6.7 and 5.6 ka.

On the coastal plain of northwest Canada, the formation of thermokarst lakes peaked between 11.6 and 10.3 ka (Rampton, 1988), suggesting maximal warmth during this interval. Thickening of the active layer between 10.3 and 9.1 ka is recorded by a widespread thaw unconformity along the Arctic coast of northwest Canada (Burn, 1997) and in the central

Yukon (Burn et al., 1986). Thermokarst collapse led to peatland development on Tuktoyaktuk Peninsula ca. 9–8 ka (Vardy et al., 1997). Finally, pigment, diatom, and sediment mineralogy of a saline lake in the central Yukon (Lake U60, site 32) indicate that temperatures and lake productivity were highest between 12.2 and 9.2 ka.

3.2. Northern continental Canada

3.2.1. Physiographic and antecedent conditions

This region spans from the Mackenzie District of the Northwest Territories east of approximately 130°W longitude to the coast of the Labrador Sea (Fig. 1), and is dominated by the low-lying Canadian Shield surrounding Hudson Bay with mountains in the westernmost district of Mackenzie and in Labrador. Almost the entire region was covered by the Laurentide Ice Sheet, which retreated northeastward across the region during the early Holocene (Dyke and Prest, 1987a).

3.2.2. Eastern Mackenzie Mountains to Hudson Bay

The broad-scale pattern of Holocene climate change in this subregion has been identified through evidence from lakes (Moser and MacDonald, 1990; MacDonald and Gajewski, 1992; MacDonald et al., 1993; Szeicz et al., 1995; Edwards et al., 1996; Wolfe et al., 1996; Pienitz et al., 1999; Szeicz and MacDonald, 2001), peat (Nichols, 1975; Kay, 1979; MacDonald, 1983), and the distribution of paleopodzols (Bryson et al., 1965; Sorenson, 1977). Many of these studies infer a climate warmer than present during the mid-Holocene (ca. 8–5 ka), resulting in increased vegetation density or a northward displacement of treeline, followed by cooling during the late Holocene (ca. 4–2 ka). The timing of maximum warmth in central Canada varied across the region (Fig. 4) and lagged eastern Beringia and northwest Canada. Analysis of pollen and macrofossils from Natla Bog (site 43; Fig. 4a) and lake cores from the Mackenzie Mountains (western NWT; sites 44–46) indicates an advance of the *Picea* treeline to positions slightly higher than the modern treeline between about 8.0 and 7.0 ka, and a retreat after about 4.0 ka. Farther east on the Canadian Shield, pollen and diatoms from Queen's and Toronto lakes (central NWT; sites 59 and 60) show a period of rapid forest–tundra expansion 6.0–3.5 ka, similar to other sites near treeline northeast of Yellowknife (Moser and MacDonald, 1990; MacDonald et al., 1993; Fig. 4b). Diatom, isotopic, geochemical, and sediment records from these treeline lakes indicate that the period of treeline advance coincided with changes in lake ecosystems. Lake productivity and dissolved organic carbon increased, pH decreased, and the δ^{18}O decreased as effective moisture increased (MacDonald et al., 1993; Edwards et al., 1996; Pienitz et al., 1999; Wolfe et al., 2000; Rühland, 2001). During the HTM at lake TK-20 (site 62), diatom diversity increased dramatically, with the first appearance of centric, planktonic taxa triggered by a moister and warmer climate (Fig. 4c). However, relatively low abundances of *Picea mariana* pollen suggest that spruce likely did not invade the catchment.

The δ^{18}O of organic matter from lakes in north-central Canada suggests an increase in the mean annual temperature of about 3°C between about 5.6 and 3.3 ka, with a 10–15% increase in summer relative humidity compared to present (Edwards et al., 1996; Pienitz et al., 1999; Fig. 4d). In contrast, during the early Holocene, precipitation was enriched in δ^{18}O at a time when temperatures were at least as low as present and are discordant with the isotope-temperature relation that was established after 5.0 ka, perhaps reflecting an increase in the efficiency of long-distance moisture transport.

During the HTM the permafrost zone shifted northward by about 300–500 km of its present distribution (Zoltai, 1995). This shift was associated with peatland development through thermokarst collapse, the formation of fen over poorly drained mineral soils, and peat formation over shallow ponds (Zoltai, 1995; Vardy et al., 1997). Peatlands started to develop ca. 11.6 ka in most ice-free areas of central Canada, probably in response to both warming and increased moisture (Zoltai and Tarnocai, 1975; MacDonald, 1987; Zoltai and Vitt, 1990; MacDonald and McLeod, 1996; Gajewski et al., 2001). At the southern edge of the boreal forest, peatland development was either delayed, or in some cases early Holocene peatlands were dessicated until after the HTM (6–5 ka), when effective moisture increased (Zoltai and Vitt, 1990; Hutton et al., 1994; Gajewski et al., 2001). Peatlands in central NWT are younger than 6 ka whereas those to the west, where deglaciation occurred earlier, are older than 6 ka (Zoltai, 1995). The increased dominance of *Sphagnum* marked the subsequent cooling (Zoltai, 1995; Vardy et al., 1997, 1998).

3.2.3. Quebec and Labrador

The Laurentide Ice Sheet lingered until about 6.8 ka in northern Quebec and Labrador and impacted climate in this subregion long after adjacent areas had warmed (COHMAP, 1988; Richard, 1995). Southeast Labrador may have experienced the HTM ca. 8–6 ka (Sawada et al., 1999) whereas northern sites, in regions that were deglaciated late, may have peaked as late as 3.7 ka, when *Picea* replaced *Alnus* pollen at most sites in the lichen woodland and forest tundra (Gajewski and Garralla, 1992; Gajewski et al., 1993, 1996). Pollen evidence from some treeline sites suggests a slight expansion of *Picea* treeline or increased density of taxa between 5 and 2 ka (Short and Nichols, 1977; Richard, 1981). Detailed analysis of paleosols, soil charcoal, and macrofossils

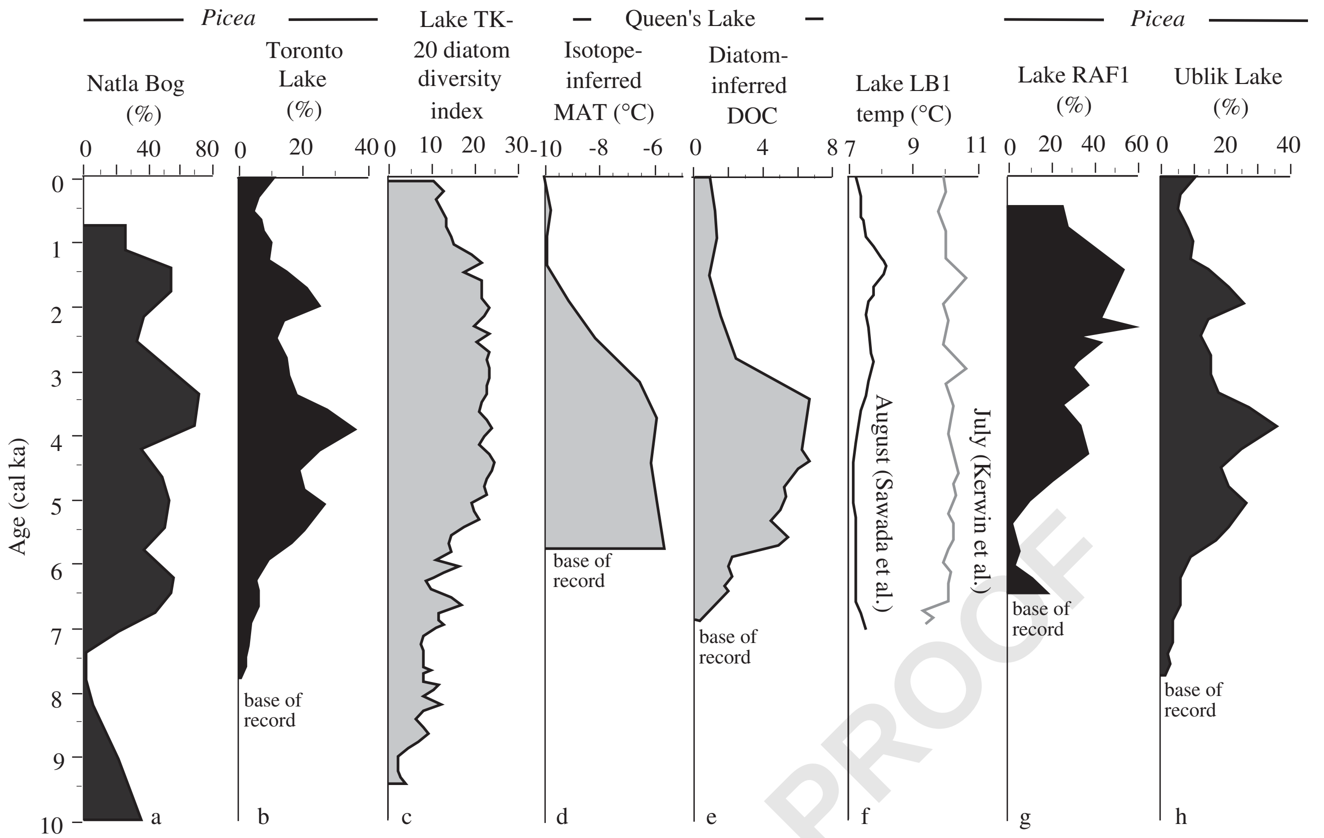

Fig. 4. Selected records of the HTM from northern continental Canada. Palynological records of tree expansion in the treeline zone are presented in black to accentuate the regionally asynchronous nature of expansion. (a) *Picea* pollen percentage, Natla Bog, Mackenzie Mountains, NWT (MacDonald, 1983). (b) *Picea* pollen percentage, Toronto Lake, NWT (MacDonald et al., 1993). (c) Diatom species diversity calculated using Hill's N2 diversity index, Lake TK-20 (Rühland, 2001). (d) Isotope-inferred change in mean annual temperature (MAT), Queen's Lake, NWT (Edwards et al., 1996; Pienitz et al., 1999). (e) Diatom-inferred dissolved organic carbon (DOC), Queen's Lake, NWT (Pienitz et al., 1999). (f) Pollen-inferred temperature, Lake LB1, Quebec, showing August temperature estimates from Sawada et al. (1999) and July temperature estimates by Kerwin et al. (submitted). (g) *Picea* pollen percentage, Lake RAF1, northern Quebec (Richard, 1981). (h) *Picea* pollen percentage, Ublik Pond, northern Labrador (Short and Nichols, 1977).

indicates a limited northward expansion of spruce in Quebec (Payette and Lavoie, 1994). Quantitative, pollen-based July temperature reconstructions (using response surface and modern analog techniques) suggest the local HTM (+2°C) took place 3.7 ka at two tundra sites (Ublik Lake and Nain Pond; sites 89 and 90) in northeast Labrador (Fig. 4f). The timing and magnitude of the HTM is less clear in tundra regions of northern Quebec. The Diana 375 Lake pollen record (site 80) suggests that the HTM (+1°C) began at 6.3 ka and was terminated by 5.0 ka. Evidence for the HTM is less apparent in the forest tundra regions of northwest Quebec, where *Picea* increased gradually (Richard, 1981; Gajewski and Garralla, 1992; Gajewski et al., 1993, 1996). Quantitative reconstructions at lake LB1 (NW Quebec; site 71) suggest that July temperatures warmed to near present immediately after the last remnants of the Laurentide Ice Sheet had melted, and peaked (+0.5°C) between 6.3 and about 2 ka (Kerwin et al., submitted; Fig. 4f). Modern-analog-based pollen methods suggest that the temperature during the HTM in this region was only slightly higher than present (+1°C; Sawada et al., 1999).

On the Labrador shelf, meltwater from the residual Laurentide Ice Sheet suppressed SSTs until the middle Holocene (Levac and deVernal, 1997; Andrews et al., 1999). For example, the Arctic freshwater benthic foraminifera *Elphidium excavatum* forma *clavata* dominated the assemblages in Cartwright Saddle (site 94) on the Labrador Shelf from ca. 12–6 ka. It then disappeared until the onset of Neoglaciation (4–5 ka).

3.3. *Canadian Arctic Islands*

3.3.1. *Physiographic and antecedent conditions*

This region spans from the west coasts of Banks and the Queen Elizabeth islands, which border the Arctic Ocean, to the east coasts of Baffin and Ellesmere islands, which rim Baffin Bay in the northwest North Atlantic Ocean (Fig. 1). In between are numerous channels and sounds, which were occupied by the Laurentide and Innuitian ice sheets. Relief increases eastward, culminating in high plateaus and fretted mountain ranges that presently support the largest ice caps in the Canadian Arctic. Isostatic uplift following deglaciation influenced the discharge of ocean currents and sea ice as the channels rebounded and shallowed during the Holocene. Most of the archipelago was deglaciated during the interval between 11.5 and 9.0 ka, but not until ca. 8 ka in the Foxe Basin–Baffin Island region and Ellesmere and Axel Heiberg islands. The terrestrial remnant of the Laurentide Ice Sheet slowly retreated toward the present-day Barnes Ice Cap (Baffin Island), which still contains residual Pleistocene ice in its lower levels (Hooke and Clausen, 1982). Because of the difference in the timing of deglaciation, the Baffin subregion is considered separately. Proxy records from ice cores and from areas that were deglaciated early show evidence of a two-fold HTM. Records from areas deglaciated later show only the later, middle Holocene maximum.

3.3.2. Arctic Islands

The interval of rapid deglaciation following the Younger Dryas (11.5–9.0 ka) was also the period of maximum Holocene warmth (Fig. 4). The strongest indication is the melt-layer record of the Agassiz Ice Cap (NW Ellesmere Island; site 77), which shows elevated percent melt between 10 and 6.5 ka, peaking between 10 and 9 ka (Fig. 5a). Maximum concentrations of pollen, particularly *Picea* and *Pinus*, are also found in the Agassiz Ice Cap during this time period (Bourgeois et al., 2000) suggesting a strengthened atmospheric circulation. In contrast, the Agassiz ice core $\delta^{18}O$ record shows a somewhat delayed maximum at 8.5 ka, possibly reflecting the depleted $\delta^{18}O$ of "recycled" Laurentide Ice Sheet meltwater and northern ocean surfaces (Fisher, 1992; Fisher et al., in press). This effect might have similarly influenced other ice-core records in the North Atlantic region, including Greenland.

The history of sea-ice cover in the Archipelago has been inferred from the distribution of more than 1000 bowhead whalebone remains (Dyke et al., 1996a; Dyke and Savelle, 2001; Fig. 5b) and walrus bones (Dyke et al., 1999) in raised marine deposits. Seasonal migrations of both animals are constrained by the patterns of ice break-up and freeze-up. Atlantic bowheads reached their maximum abundance in the channels of the eastern and central Arctic Archipelago from 11.5 to 8.5 ka, but were excluded from areas along northeastern Baffin Island. Pacific bowheads reached their maximum abundance in the western Arctic channels connecting to the Beaufort Sea at the same time. During that interval, whales extended into areas well beyond their present ranges, then retreated abruptly at about 8.5 ka. The bowhead range may have expanded as sea-ice export from the Archipelago was enhanced by abundant meltwater during the interval of rapid glacial recession. Alternatively, greater summer warmth may alone account for reduced summer sea-ice cover. Sea-salt sodium concentrations in Penny Ice Cap (SE Baffin Island; Fisher et al., 1998) and the Greenland Ice Sheet (Mayewski et al., 1997) are at highest levels in early Holocene ice (11.5–9.0 ka), consistent with minimal sea-ice cover. Bowhead whale ranges re-expanded in the middle Holocene (6–3 ka). Although the range did not attain early Holocene extent, the re-expansion was concurrent with the advance of treeline in the region to the south, the HTM in that area.

Available records indicate that molluscs did not survive the last glacial maximum in continental shelf waters in the western Arctic Ocean. With submergence of Bering Strait ca. 13 ka, cold-water-tolerant molluscs *Hiatella arctica* and *Portlandia arctica* entered the western Arctic Ocean. At 11.5 ka, two boreal-subarctic thermophiles, *Mytilus edulis* and *Macoma balthica*, then spread from Bering Strait along the Beaufort Sea coast at least as far as the modern limit of *M. edulis*, coincident with the entry of Pacific bowheads. These thermophilous molluscs require summer SSTs above 0°C for successful dispersion of larvae. Thus, SST rose above current values immediately following 11.5 ka and the abundance of dated thermophilous molluscs from the Canadian archipelago reached a maximum during the interval 11.5–8.5 ka (Fig. 5c). *M. balthica* then withdrew from the western Arctic during the late Holocene.

3.3.3. Baffin Island and Baffin Bay region

The record of thermophilous molluscs in the Baffin Bay area indicates changes in coastal marine conditions during the early Holocene (Andrews, 1972; Fig. 5c). Molluscs first reached their modern limit in eastern Baffin Bay at 10.0 ka, thus signaling the establishment of the West Greenland Current, the only warm current in the region (Funder and Weidick, 1991; Dyke et al., 1996b). Shortly thereafter, boreal-subarctic molluscs extended along the east coast of Baffin Island, as much as 1000 km north of their modern limits; records are insufficient to establish the timing of the HTM. However, two boreal molluscs, *Panopea norvegica* and *Arctica islandica*, occupied southeastern Baffin Bay by 9.4 ka, then withdrew prior to 4.5 ka (Funder and Weidick, 1991), thus defining the interval of maximum warming of the West Greenland Current. Retraction to modern limits along the east coast of Baffin Island occurred as the Baffin Current cooled about 3 ka. Similarly, dinoflagellates in northern Baffin Bay indicate that SST reached close to modern as early as 9.6 ka, and

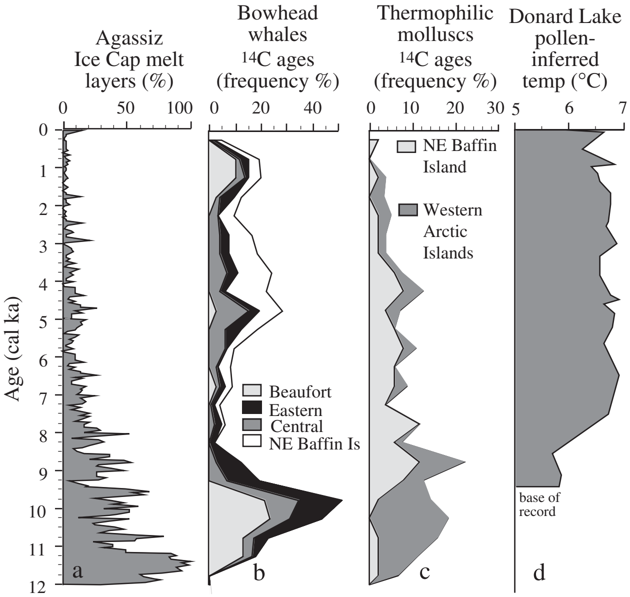

Fig. 5. Selected records of the HTM from the Canadian Arctic Islands. (a) Melt record, Agassiz Ice Cap, northern Ellesmere Island showing the percentage of annual layers in a 50-year interval that contains ice formed by melting near the surface in summer; the record assumes no change in snow accumulation rate (Fisher and Koerner, 2003). (b) Occurrence of bowhead whale bones based on frequency distribution of ^{14}C ages (bin size = 500 yr) in four areas: (1) Beaufort Sea (70.1±0.6°N latitude, 116.6±1.5°W longitude, $n = 38$), (2) northeastern islands (75.2±0.9°N latitude, 86.9±3.6°W longitude, $n = 98$), (3) central islands (72.6±1.1°N latitude, 94.2±4.8°W longitude, $n = 118$), and (4) northern Baffin Island (71.9±0.6°N latitude, 85.1±2.2°W longitude, $n = 204$) (data compiled by A.S. Dyke; available at PARCS website). (c) Occurrence of thermophilic molluscs based on the frequency distribution of ^{14}C ages (bin size = 500 yr) in two areas: (1) northeastern Baffin Island (70.1±1.6°N latitude, 71.6±5.4°W longitude, $n = 53$, mean±1σ) and (2) western Arctic Islands (69.4±1.4°N latitude, 114.0±3.6°W longitude, $n = 66$) (data compiled by A.S. Dyke; available at PARCS website). (d) Pollen-inferred summer temperature, Donard Lake (Kerwin et al., submitted).

was higher than present between 6.4 and 3.6 ka (Levac et al., 2001).

The Baffin Bay thermophilic molluscs did not extend into the central archipelago. Their farthest northwest occurrences were in Navy Board Inlet (NW Baffin Island), Smith Sound (SE Ellesmere Island), and adjacent Greenland. This distribution, and the absence of the West Greenland Current before 10 ka, constrains our interpretation of warming within the archipelago during the HTM. The extended bowhead range 11.5–9.0 ka requires greater summer sea-ice clearance than occurs today, hence temperatures above the –1.8°C freezing point of sea water. But the failure of thermophilic molluscs to enter suggests that summer SST did not rise much, if any, above 0°C.

The longest well-dated pollen records from the region are from easternmost Baffin Island. Donard Lake (site 91; Fig. 5d) shows a three-step warming: initial warming at 14.4 ka, a second step dominated by grass pollen beginning ca. 12 ka, and a final step about 9 ka. Glaciers advanced at 9.5–8.6 ka, and again at ca. 5.7 ka continuing to the present (Moore, 1996; Moore et al., 2001). Maximum pollen accumulation rates (partly exotic taxa) occurred between 8.6 and 5.7 ka, presumably representing the local HTM. Peak warmth at 6 ka is estimated at +1°C for Donard Lake, and for nearby Fog (site 88) and Dyer Lower lakes (site 92), based on unpublished pollen records (Kerwin et al., submitted). At Robinson Lake (site 87), organic sedimentation began ca. 12.1 ka, grass tundra was succeeded by sedge tundra at 9 ka, and maximum pollen accumulation occurred 9–5 ka, as at Donard Lake. This zone might represent the HTM, or it might mainly record exotic pollen influx from Quebec–Labrador. The possibility that local pollen (and thus the local HTM) is obscured is further indicated by diatoms from Donard and Robinson lakes, as well as from Amarok Lake (site 85), a tarn with a basal age >11.3 ka. Organic sedimentation rate and diatom productivity indicate that the HTM was 10.2–9.3, earlier than suggested by the pollen (Wolfe, 1994, 1996).

Two lakes on Somerset Island (lakes RS29 and RS36; sites 64 and 65) that were deglaciated about 10.3 ka have maximum pollen accumulation rates between 10.3 and 6.0 ka, suggesting maximum plant density on the landscape at that time. Similarly, a lake on Prince of Wales Island (Lake PWWL, site 63) contains maximum pollen concentrations before 5 ka. Farther west, on Banks Island, four relatively poorly dated pollen records (sites 50–53) with basal ages of about 9 ka indicate maximum temperatures between 7 and 2 ka. On Ellesmere Island, algal populations from lake sediments are largely controlled by the extent of summer lake-ice cover (Smol, 1983, 1988; Smith, 2002). For example, diatom and pollen records from Rock Basin Lake (site 69) indicate higher temperatures from about 8.4 to 4.5 ka. An increase in diatom concentrations beginning about 5.5 ka and peaking at 3.5 ka marks a later local HTM at several lakes in the Lake Hazen area (NE Ellesmere Island; site 82), where warm conditions continued until about 2.0 ka. This area was not deglaciated until 8.4–6.8 ka, contributing to the delayed warming in comparison with Rock Basin Lake.

3.4. Greenland and Iceland

3.4.1. Physiographic and antecedent conditions

This region includes Greenland and Iceland and their relatively narrow continental shelves (Fig. 1). Greenland spans the entire latitudinal range of the North American Arctic. It supports the single remaining ice sheet in the Arctic, from which premier paleoclimate records have been extracted. The ice sheet cools the region through its self-sustaining influence on atmospheric circulation, sea-surface salinity, and energy balance. It also responds dynamically to climatic changes, through both temperature and accumulation forcing (Cuffey and Clow, 1997).

The climate of this region is also influenced by ocean currents in the Labrador and Greenland seas (Fig. 1). The northward-flowing North Atlantic Current bifurcates around Iceland. The western branch (the Irminger Current) flows into Denmark Strait and converges with the southward-flowing East Greenland Current. They join and flow westward to form the West Greenland Current, which flows into Baffin Bay and joins the southward-flowing Labrador Current. The convergence of warm, subtropical water with cold polar water, gives rise to high precipitation rates in southern Greenland and cold continental temperatures that promote glacerization. In this region, climate is not only influenced by changes in ocean circulation, but can itself influence the entire globe through changes in the production of deepwater in the North Atlantic Ocean (Broecker and Denton, 1989), including abrupt changes on decadal timescales (Clark et al., 2002). During the early Holocene, this region was strongly impacted by the waning Laurentide Ice Sheet, which transmitted its effect to key areas of ocean convection through both the atmosphere and the ocean.

3.4.2. Greenland

In general, peak warmth in Greenland appears to have occurred between 9 and 5 ka, depending on which temperature proxy is considered (Fig. 6). Borehole temperature inversions from the GRIP (site 109/110) and Dye 3 (site 105) ice-core sites show maxima between 8 and 5 ka, and 6 and 3 ka, respectively (Fig. 6a). The isotope profile from North GRIP (site 106) and borehole-temperature-calibrated isotope data from GISP2 (site 108) suggest somewhat earlier and smaller amplitude maxima (Fig. 6b). Dye 3, located at lower elevation, closer to the ocean, and to the southwest, shows at least twice the amplitude of change compared with the Greenland summit (Buffey and Clow, 1997: Dahl-Jensen et al., 1998). Thus, the magnitude of HTM warmth was likely greater in southwest Greenland, and at lower elevations or closer to the ocean than at the summit or at higher latitudes.

Lacustrine evidence also suggests that warming and subsequent cooling were spatially variable across Greenland (Fredskild, 1992; Anderson et al., in press). In south Greenland, the HTM took place between ca. 8 and 2 ka (Fredskild, 1973), with warmest conditions ca. 7.5 ka (Fredskild, 1984). In the Godthåbsfjord area (site 103), evidence for the HTM is equivocal, but was probably associated with a rise in *Betula nana* and *Juniperus* pollen between 7 and 4 ka (Fig. 6c), and as recently as 3.5 ka at one site (Terte Lake A, site 97). At Qipisarqo Lake (site 104), the HTM peaked 6 ka and lasted until about 3 ka, on the basis of biogenic silica and organic carbon concentrations (Fig. 6d) (Kaplan et al., 2002). However, chironomid assemblages from this lake suggest a much earlier HTM (9–7 ka) and the possibility that catchment evolution exerted an equally strong control on primary productivity in the lake as did summer temperature (Wooller et al., in review; Fig. 6e).

In west Greenland, the thermophilic ostracode *Ilyocepris bradyi* indicates a period of maximum water temperature between 7.0 and 6.5 ka (St Salt Sø, site 101). Lake-water conductivity inferred from diatom assemblages in two nearby, closed-basin, oligosaline lakes (lakes SS6 and Bray Sø; sites 98 and 99) suggests high evaporation rates between 8 and 5 ka, presumably reflecting greater warmth. $\delta^{18}O$ analyses from the same lakes indicate considerable evaporative enrichment ca. 7 ka whereas chironomid-inferred temperatures for lake SS2 (site 100) show no major trend during the Holocene, despite substantial changes in chironomid species abundance (N.J. Anderson, K.P. Brodersen, and M.J. Leng, unpub. data). Glacial fluctuations and extralimital subarctic molluscs along the west coast of Greenland indicate that the HTM occurred between ca. 8.0 and 3.5 ka (Kelly, 1980). The ages of extralimital boreal taxa, however, are generally older (Funder and Weidick, 1991), indicating warmest nearshore temperatures between ca. 10.5 and 6 ka (Fig. 6f).

Relatively few lake-sediment records have been recovered from east Greenland. Biogenic silica concentrations and diatom assemblages indicate that the HTM occurred between 9 and 6 ka at Lake Basaltsø (site 121; Fig. 6g). This agrees with the occurrence of thermophilic molluscs along the east coast (Fig. 6f; Hjort and Funder, 1974) and marine records from off the Greenland east coast. The percentage of *B. nana* pollen in lake N1 (Ymer Island, site 118) places the HTM at 7.7–5.0 ka.

The HTM in north Greenland was quite different, with warmer but drier conditions prevalent until 5 ka (Fredskild, 1984). On the Cary Islands, peat was deposited between ca. 6.5 and 4.5 ka and is interpreted to represent the HTM (Brassard and Blake, 1978).

Because thermophilic plants did not survive in Greenland during the last glacial maximum, their immigration was delayed by the lack of a terrestrial connection. The later initiation of the HTM inferred from ecological indicators in lake sediments from some localities, compared with records offshore (see below), may reflect the lag associated with colonization. Lake sediments tend to indicate a more variable early Holocene than do ice cores, which may reflect the influence of catchment processes, lake development, and the sensitivity of lakes to regional climate development (Anderson et al., in press). On the other hand, sediment carbon content at lake NAUJG1 (site 96; Fig. 6h) in west Greenland is strongly correlated with proxies from the ice-core record, supporting the association between organic production and regional climate.

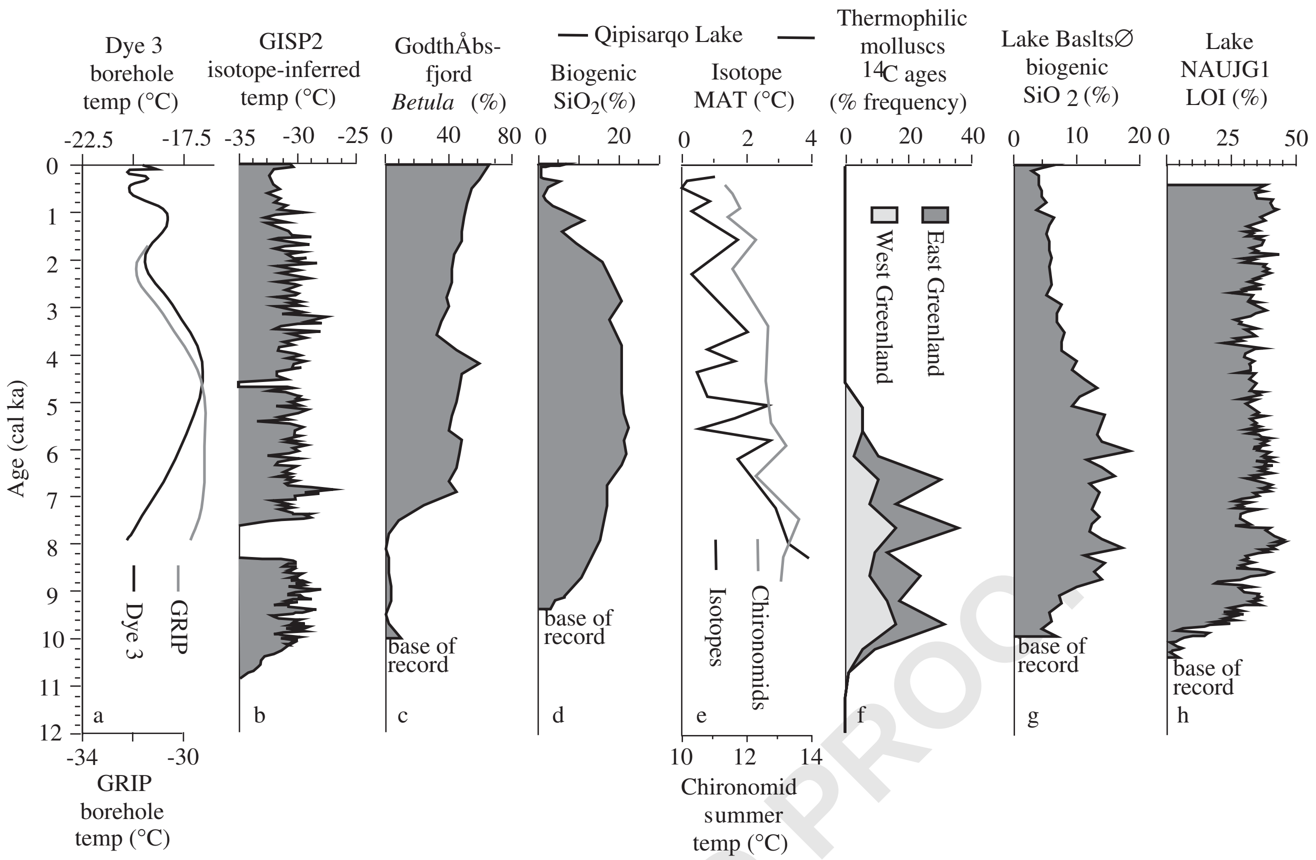

Fig. 6. Selected records of the HTM from Greenland and Iceland. (a) Temperatures inferred from inverse-modeled borehole temperatures at Dye 3, southwest Greenland, and Summit (GRIP), central Greenland (Dahl-Jensen et al., 1998). (b) Isotope-inferred temperature calibrated using borehole temperature, GISP2, central Greenland (Cuffey et al., 1995). (c) *Betula* pollen percentage, Godthåbsfjord (Fredskild, 1973). (d) Biogenic silica, Qipisarqo Lake, southwest Greenland (Kaplan et al., 2002). (e) Mean annual temperature (MAT) inferred from the oxygen-isotope composition of chironomids, and summer lake-water temperature inferred from chironomid assemblage transfer function, Qipisarqo Lake (Wooller et al., in review). (f) Occurrence of thermophilic mollusc shells based on frequency distribution of ^{14}C ages (bin size = 500 yr) for: (1) east Greenland (67.2 ± 1.0°N latitude, 52.5 ± 1.5°W longitude, $n = 77$), and (2) west Greenland (72.1 ± 1.5°N latitude, 24.3 ± 1.3°W longitude, $n = 26$) (data compiled by A.S. Dyke; available at PARCS website). (g) Biogenic silica, Lake Basaltsø (Wagner et al., 2000). (h) Loss-on-ignition (LOI), Lake NAUJG1 (Willemse and Törnqvist, 1999).

Offshore, on the east Greenland shelf (site 114), the HTM began after the influence of meltwater declined at ca. 10.9 ka. The HTM is recognized as the interval of lowest ice-rafted detritus (IRD) content and highest percentages of *Cassidulina neoteretis*, a benthic foraminifera species inhabiting slightly modified Atlantic Intermediate Water. This occurred from 9 to 5 ka, with peak warmth (lowest IRD) possibly between 7 and 5 ka, concurrent with the retreat of the Greenland Ice Sheet behind its present margins (Funder, 1989). Warming and subsequent cooling occurred earlier on the east Greenland margin south of the Denmark Strait (site 111) compared with north of the strait (site 115). By 7 ka, the modern circulation regime was established, with the East Greenland Current dominating the shelf. The HTM appears to have ended relatively abruptly in many areas of the North Atlantic region with an interval of increased particle-size sedimentation ca. 5.7 ka (Steig, 1999; Bond et al., 2001), which occurred during an interval of high δ^{18}O values (cold or salty conditions, or both) in North Iceland benthic foraminifera (Andrews and Giraudeau, 2003; Castaneda et al., 2003). At about the same time, sites on the east Greenland margin are marked by a strong influx of IRD (Andrews et al., 1997; Jennings et al., 2002).

3.4.3. Iceland

Presently, there are no continuous records of climatic evolution that span the Holocene from Iceland. Although little quantitative data are available, Iceland is generally thought to have experienced longer, warmer summers during the early Holocene. Most records are based on either glacial geomorphology, which is episodic, or on vegetation change over a limited time, which is difficult to evaluate in the context of long-term ecosytem evolution. The most complete record in

Northern Iceland is from a treeline site (Vesturárdalur, site 131), where macrofossils indicate that *Betula* expanded to near its maximum Holocene distribution by 8.6 ka. A distinct maximum of *Betula pubescens* and pollen accumulation rates between ca. 7.5 and 6.7 ka suggests a later HTM, however. This is in accordance with results from Vatnskotsvatn (site 129), where a *Betula* forest was established between 9.7 and 5.6 ka and pollen influx peaked around 7.8 ka. In southern Iceland (Lómatjörn, site 126), *Betula* pollen appeared just after 8.9 ka, with forests inferred to have been most dense between 8.1 and 5.6 ka. In northwest Iceland (Efstadalsvatn, site 120), a chironomid-based reconstruction indicates highest summer temperatures ca. 9.1 ka; temperature continued to rise there until 4.4 ka. The earlier warming is consistent with the marine record from the adjacent continental shelves (see below), indicating a lag between the onset of warmth and the establishment of *Betula*.

The evolution of Holocene climate has been studied offshore of Iceland (e.g., Hagen, 1995; Eirîksson et al., 2000). Carbonate accumulation, a measure of net marine productivity, clearly indicates early Holocene warmth, with maximum values around 5–4 ka (Andrews et al., 2001; Andrews and Giraudeau, 2003). Sediment from Gardar Drift south of Iceland (site 117) records the influence of the North Atlantic Drift after 11.2 ka. Coccolith assemblages indicate that the site warmed progressively from 10 to 6 ka, with SST reaching +2–3°C between 7 and 6 ka. Subsequent to 6 ka, cooling coincided with increased freshwater advection. North of Iceland (site 123), the HTM occurred between 9.0 and 6.2 ka, peaking at 7.0 ka on the basis of $\delta^{18}O$ composition of benthic forams. Coccolith species assemblages indicate that Atlantic Water was present from 10.0 to 6.2 ka. Faunal changes at sites north of Iceland show that the HTM occurred between 10.3 and 6.7 ka (Eirîksson et al., 2000; Jiang et al., 2002). Similarly, cores from fjord and shelf settings northwest of Iceland contain carbonate evidence for the HTM between 10.3 and 6.7 ka (Geirsdóttir et al., 2002; Andrews et al., 2003). Both the terrestrial and the marine records reflect cooling and fluctuating conditions beginning 6.7 ka, a dramatic decrease in pollen content around 6.1 ka, and a further decline in both records around 3.3 ka.

3.5. Summary: spatio-temporal pattern of the HTM, western Arctic

At the 120 sites across the western Arctic that reported evidence for the HTM, the warmest interval (primarily based on indicators of summer temperature) of the Holocene began on average 8.9±2.1 ka (mean±1σ; median = 9.0 ka) and ended 5.9±2.6 ka (median = 6.0 ka). The large standard deviation associated with the timing of the HTM is indicative of the strong spatial heterogeneity of this time-transgressive even, and is clearly expressed by maps of HTM initiation and termination isochrons (Fig. 7). Much of the variability is longitudinal (Fig. 8). Eastern Beringia clearly warmed earlier than northern continental Canada; nearly all sites where warming took place prior to ca. 11 ka are in Alaska, whereas sites where the HTM was significantly later (after 7 ka) are in the central interior of Canada surrounding Hudson Bay. On average, sites in central and eastern Beringia experienced the HTM by 11.3±1.5 ka ($n = 25$) (Table 2); some sites ($n = 15$), mainly in central Beringia, do not reveal palynological evidence for warmer-than-present conditions anytime during the post-glacial interval. In contrast, the HTM in northern continental Canada was delayed until 7.3±1.6 ka ($n = 22$), with an additional three sites lacking clear evidence for the HTM. The timing of the HTM was generally similar among sites in both marine and terrestrial settings (Table 2). Taken together, HTM conditions in the Canadian Arctic Islands and the Greenland–Iceland regions, were reached 8.6±1.6 ka, with all but two sites reporting clear evidence of an HTM.

Regions tended to cool in the order that they warmed. The HTM ended first in central and eastern Beringia (9.1±2.0 ka), then in Greenland–Iceland (5.4±1.4 ka), the Canadian Arctic Islands (4.9±2.6 ka), and finally in northern continental Canada (4.3±2.2 ka). The duration of the HTM tended to be shorter in central and eastern Beringia than in other regions of the western Arctic. On average, it lasted 2200±1300 yr in central and eastern Beringia, compared with 3100±1700 yr in northern continental Canada, and 3400±1400 in the Canadian Arctic Islands and Greenland–Iceland. The standard deviations for the timing of HTM terminations both within and between each of the four regions are about 20% higher than the standard deviations for the timing of the initiation, suggesting that the cooling was more variable than the warming. This is counterintuitive considering that the onset of the HTM in the North Atlantic region was interrupted by abrupt meltwater releases from the decaying Laurentide Ice Sheet whereas, during the later part of the Holocene, geography was similar to present and the disruptions by the ice sheet were absent.

Quantitative estimates of the magnitude of temperature increase during the HTM have been reported at only 16 terrestrial and coastal sites and eight open-marine sites in the western Arctic (Table 3). Despite the variety of approaches used, all estimates from terrestrial sites fall within the narrow range of 0.5–3°C and average 1.6±0.8°C. Marine sites recorded more than twice the increase in temperature during the HTM (3.8±1.9°C; $n = 9$).

4. Causes of the HTM and its spatio-temporal pattern

4.1. Direct forcing and climatic feedbacks

Broadly speaking, early Holocene warmth was driven by earth's orbital variations. Precessional forcing culminated 12–10 ka, when total annual insolation was $1\,\mathrm{W\,m^{-2}}$ higher than present at 60°N, and $5\,\mathrm{W\,m^{-2}}$ higher at the pole (Berger and Loutre, 1991). At that time, insolation at 60°N during summer (June) was 10% higher than today, and only slightly lower during winter (December) (Fig. 9).

Compared to the increase in summer insolation, radiative forcing by changes in atmospheric trace-gas concentrations was minor during the early Holocene. CO_2 attained concentrations near its pre-industrial level by about 11 ka and remained constant during the early Holocene (Indermühle et al., 2000), while CH_4 decreased slightly (Blunier et al., 1995) (Fig. 9). In contrast, as the climate warmed, the water-vapor content of the atmosphere probably increased (e.g., Foley et al., 1994), and the flux of heat and moisture from the tropics to the Arctic probably strengthened, resulting in a positive feedback on warming. As it appears to have done over the latter part of the 20th century (Folland et al., 2001), the pattern of increased atmospheric water vapor probably mirrored that of temperature.

Climatic feedbacks of radiative forcing during the early Holocene were spatially variable. The extent of snow and ice cover was reduced and the pattern of vegetation cover was altered. Both impacted the distribution of energy absorbed during the summer, and altered the surficial energy and water balances sufficiently to carry into the fall and winter months. Feedbacks involving the reduction in glacier and sea-ice extent were particularly significant for high-latitude amplification of warming. Vegetated land and open sea have much lower albedo and a higher heat capacity than ice. As ice cover decreased and summer insolation increased, more solar energy was stored in summer and then re-radiated during the winter (e.g., Gildor and Tziperman, 2001). Year-round warming was also likely facilitated by the expansion of forests over tundra, further reducing surface albedo and leading to a positive feedback (Foley et al., 1994; Chapin et al., 2000). The positive feedback on temperature by land-surface changes probably had a distinct spatial pattern, with earlier and larger responses occurring in regions where snow cover was low and vegetation was readily converted from steppe or tundra to high shrub or forest, as in Beringia. The distribution of sea ice in response to circulation changes also contributed to the spatial pattern of warming. Simulations of 6 ka climate by GCMs with a dynamical sea-ice routine show a thickening of sea ice in the western Arctic and a thinning in the eastern Arctic (Vavrus, 1999; Vavrus and Harrison, in press), suggesting a negative feedback on surface-temperature response to insolation forcing. Although the geography of boreal-forest expansion (MacDonald and Gajewski, 1992) and glacier-ice retreat (Dyke and Prest, 1987a, b) during the early Holocene are relatively well known for the western Arctic, no detailed reconstructions of sea-ice extent are yet available (Smith et al., 2003). The extent to which the warming during the HTM can be attributed to these various feedbacks is the topic of ongoing modeling research (e.g., TEMPO, 1996).

Superposed on the relatively slow changes in incoming solar radiation and atmospheric composition, higher-frequency variations in solar output, and volcanic activity affected the radiative forcing during the early Holocene (e.g., Nesje and Johannessen, 1992). For example, millennial-scale variations in the delivery of ice-rafted detritus to the North Atlantic Ocean (Bond et al., 2001), of sea-salt content of the Greenland Ice Sheet (O'Brien et al., 1995), and the grain size of magnetic minerals in marine sediment off northern Iceland (Andrews et al., 2003) seem to correspond with changes in solar irradiance, as inferred from cosmogenic isotope (^{10}Be and ^{14}C) records from ice cores and tree rings. At the millennial timescale, the amplitude and duration of the climate response to solar forcing was probably small (Cubasch et al., 1997; Viau, 2003), at most a few $\mathrm{W\,m^{-2}}$ (Stuiver et al., 1995). Similarly, volcanic forcing operated on shorter temporal scales than insolation forcing, and was more regional in scope (e.g., Zielinski et al., 1994; White et al., 1997; Briffa et al., 1998; Gervais and MacDonald, 2001).

4.2. The Laurentide Ice Sheet

Eastern Beringia generally responded in-phase with the summer insolation anomaly whereas sites in northeast North America attained their local HTM several thousand years later. The delay in the northeast can be attributed, at least in part, to the impact of the residual Laurentide Ice Sheet on the coupled oceanic and atmospheric circulation in the North Atlantic sector. The thermal inertia of the Laurentide Ice Sheet, and other residual ice masses, and its topographic expression, affected climate as downstream areas were cooled by advection through the atmosphere, and by meltwater and iceberg discharge into the adjacent seas. The ice lingered well after peak summer insolation, with the final collapse of the Foxe Basin dome about 7.5 ka (Andrews, 1989). The impact of melting ice on ocean convection persisted even after the removal of ice from major calving margins 9–8 ka (Andrews, 1987; Dyke et al., 2002). Freshwater was conveyed to the adjacent seas, including the Arctic Ocean, via meltwater runoff and drainage of massive proglacial lakes that fringed the retreating ice sheet (Andrews, 1987; Dyke and Prest,

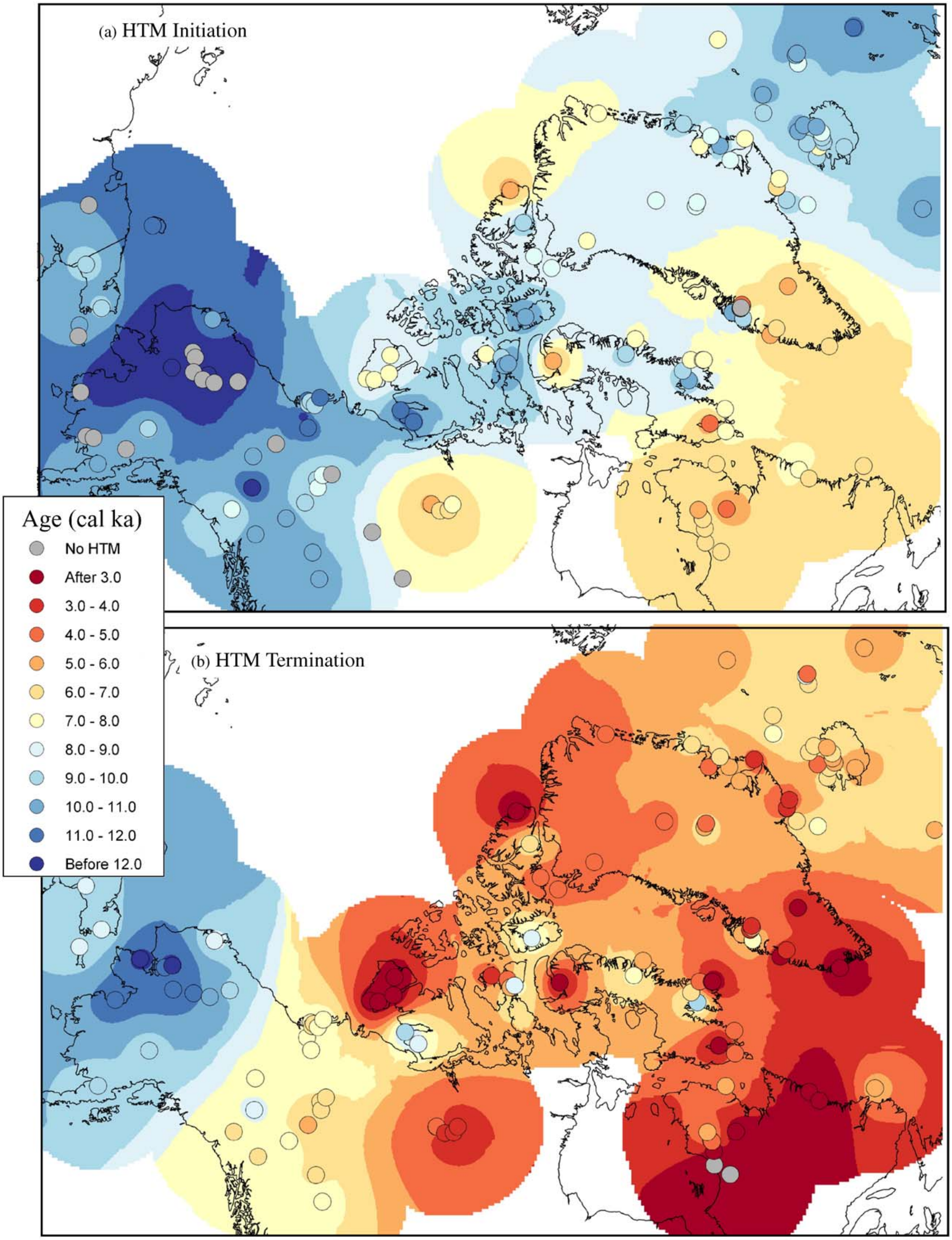

Fig. 7. Spatio-temporal pattern of HTM in the western Arctic. (a) Initiation and (b) termination of the HTM. Gray dots indicate equivocal evidence for the HTM. Dot colors indicate bracketing ages of the HTM, which are contoured using the same color scheme. Sites are listed in Table 1. These maps with references to each site and additional information are available at the PARCS website.

1987a, b; Barber et al., 1999; Licciardi et al., 1999; Fisher et al., 2002; Leverington et al., 2002; Teller et al., 2002). For example, North Atlantic cooling centered around 8.2 ka, and attributed to the drainage of ice-dammed lakes in the Hudson Bay region (Alley et al., 1997), is reflected in the overall frequency distribution of the ages of HTM initiation (Fig. 8). Sites tended to reach their local HTM either before or after this event.

GCMs help quantify the effect of residual Laurentide Ice Sheet on the atmospheric circulation. Sensitivity tests show that the simulated 9-ka ice sheet counteracted insolation-induced warming by 2°C over northeast North America and downstream over the North Atlantic (Kutzbach and Guetter, 1986; COHMAP, 1988; Mitchell et al., 1988). Similarly, more recent modeling (Pollard et al., 1998; CAPE, 2001) shows that anticyclonic circulation persisted at 10 ka, despite the retracted Laurentide Ice Sheet, and that the polar jet was displaced southward over the North Atlantic Ocean, influencing climate in the northern US (Kirby et al., 2002). The expansion of *Betula* from west to east across Alaska and northern Canada might reflect the "upstream" influence of the waning Laurentide Ice Sheet. First, its influence on circulation diminished, allowing a moister, westerly flow from the Pacific Ocean to resume. Second, the direct cooling effect of the ice migrated eastward as the ice sheet melted (Bartlein et al., 1992; Edwards and Barker, 1994). The high proportion of tree pollen in the Agassiz ice core (Bourgeois et al., 2001) may also be a reflection of this circulation.

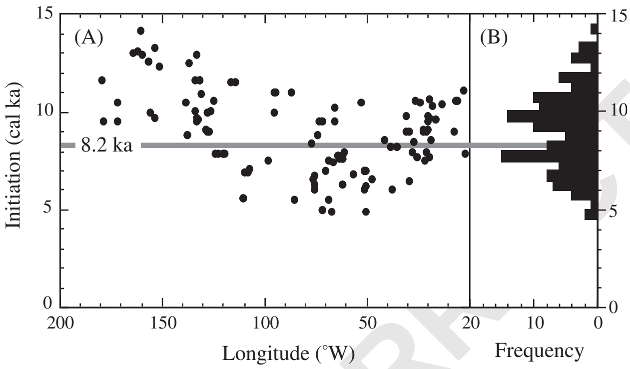

Fig. 8. Longitudinal distribution of the initiation of the HTM showing the frequency distribution of sites according to age.

Early Holocene ice sheets of northeast North America further affected climate by altering the exchange of water between the Arctic and North Atlantic oceans. During the early Holocene, the Laurentide and Innuitian ice sheets blocked the Canadian High Arctic channels (Dyke, 1999; Dyke et al., 2002), implying an increased flux of Atlantic Water through Fram Strait to conserve the mass balance. Areas under the direct inflow of Atlantic Water warmed earliest, by 10 ka, and most dramatically, by up to 5°C (Koç et al., 1993). The increased advection of warm Atlantic Water into the Arctic Ocean during the earliest Holocene could have contributed to the increased melting on the Agassiz Ice Cap (Fisher et al., 1995; Fisher and Koerner, 2003), the presence of the bowhead whales (Dyke and Savelle, 2001), and the expansion of forests in northwest Canada (Ritchie et al., 1983). It also suggests a stronger-than-present flux of modified Atlantic Water along the east Greenland margin (Koç and Jansen, 1994; Jennings et al., 2002). Farther east, a stronger-than-present flow of warm Atlantic Water is also evident by 10 ka along the north coast of Scandinavia (CAPE, 2001).

As the ice sheets melted, their mass was transferred to the ocean, resulting in local isostatic and global eustatic effects. At some sites in Beringia, for example, the HTM may have been terminated as marginal seas transgressed their continental shelves. Within the limits of Pleistocene ice sheets, delayed isostatic rebound may have altered ocean circulation. In the Canadian Arctic, channels were 100–150 m deeper than present (Andrews et al., 1991) allowing modified Atlantic Water to have flowed into Baffin Bay. Molluscan fauna indicative of warmer water are reported for this interval, but it is unclear whether this is due solely to the modified Atlantic Water from the Arctic Ocean or whether it reflects increased advection of Irminger Current water via the West

Table 2
Summary statistics for the timing of initiation and termination of the Holocene thermal maximum, and its duration, in regions across the western Arctic

Region	Initiation (cal ka)		Termination (cal ka)		Duration ($\times 10^3$ yr)		Total (*n*)	Lacks evidence (*n*)
	Mean	1σ	Mean	1σ	Mean	1σ		
Central-eastern Beringia	11.3	1.5	9.1	2.0	2.2	1.3	25	15
Northern continental Canada	7.3	1.6	4.3	2.2	3.1	1.7	23	3
Canadian Arctic Islands	8.6	1.8	4.9	2.6	3.7	1.5	27	0
Greenland–Iceland	8.6	1.5	5.4	2.0	3.2	1.3	45	2
Arctic Islands + Greenland–Iceland	8.6	1.6	5.2	2.0	3.4	1.4	72	0
Greenland–Iceland, terrestrial	7.9	1.3	5.0	1.3	3.0	1.0	26	2
Greenland–Iceland, marine	9.5	1.3	6.1	1.3	3.5	1.5	19	0

Table 3
Increase in summer temperature, relative to average 20th century conditions, during the Holocene thermal maximum

Location[a]	Lat. (°N)	Long. (°W)	Climate proxy	Peak (cal ka)	Temp. (°C)	Citation for temp. estimate
Terrestrial sites						
Alaskan coastal plain	69.7	154.9	Insect fauna	10.8	2–3	Nelson and Carter (1987)
Sleet Lake, NWT	69.3	133.8	Spruce pollen, macros	9.7	3	Ritchie (1984)
Queen's Lake, NWT	64.1	110.6	Stable isotopes	5.0	3[b]	Wolfe et al. (1996)
Lake LB1, Quebec	57.9	75.6	Pollen	3.0	0.5	Kerwin et al. (submitted)
Lake LR1, Quebec	58.6	75.3	Pollen	5.0	0.5	Sawada et al. (1999)
Diana 375 Lake	61.0	70.0	Pollen	5.8	1	Kerwin et al. (submitted)
Patricia Bay Lake	70.5	68.5	Pollen	7.4	1	Kerwin et al. (submitted)
Hikwa Lake	63.3	67.4	Pollen	3.4	2	Kerwin et al. (submitted)
Fog Lake	67.2	63.3	Pollen	5.7	1	Kerwin et al. (submitted)
Donard Lake	66.7	61.8	Pollen	5.7	1	Kerwin et al. (submitted)
Dyer Lower	66.6	61.7	Pollen	5.7	1	Kerwin et al. (submitted)
Agassiz, Ellesmere Is	80.7	73.1	Ice core melt layers	9.0	2	Koerner and Fisher (1990)
GISP2, Summit Greenland	72.6	38.5	Borehole temperature	7.7	1–2	Cuffey and Clow (1997)
GRIP, Summit Greenland	72.6	37.6	Borehole temperature	6.0	2	Dahl-Jensen et al. (1998)
Dye 3, SW Greenland	65.2	43.8	Borehole temperature	4.5	2	Dahl-Jensen et al. (1998)
Vesturárdalur, N Iceland	65.8	18.7	Pollen, macros, LOI	7.1	1.5	Wastl et al. (2001)
Marine sites						
Central Arctic Archipelago	73.6	86.0	Whales and molluscs	9.5	1	Dyke and Savelle (unpub)
MD95-2015, Gardar Drift	58.8	26.0	Coccoliths	6.5	2–3	Giraudeau et al. (2000)
MD99-2269, Iceland Shelf	66.6	20.9	Diatoms	7.9	6.6	Andrews et al. (2002)
PS21842-5, Iceland Plateau	69.5	16.5	Diatoms	8.5	6	Koç et al. (1993)
HM57-15, Iceland Plateau	69.4	13.1	Diatoms	7.9	5	Koç et al. (1993)
MD95-2011, Norwegian Sea	67.0	7.6	Diatoms	8.6	4.5	Birks and Koç (2002)
HM57-14, Norwegian Sea	67.0	6.2	Diatoms	None	3.5	Koç et al. (1993)
HM79-26, Norwegian Sea	66.9	5.9	Diatoms	None	4	Koç et al. (1993)
HM94-13, Greenland Basin	71.6	1.6	Diatoms	None	2.5	Koç et al. (1993)

[a] Additional information at the PARCS website.
[b] Mean annual air temperature; others are primarily summer temperature estimates.

Greenland Current (Andrews, 1973; Dyke and Peltier, 2000).

Although the residual Laurentide Ice Sheet profoundly affected the climate of northeast Canada and the North Atlantic region during the early Holocene, its influence is difficult to separate from climatic factors that enabled the ice sheet to linger under conditions of increasing summer insolation. Persistent glacier cover, such as that over Labrador and Quebec (Dyke and Prest, 1987a, b) that lasted well into the Holocene, may have owed its existence to Holocene atmospheric dynamics and increased precipitation at the end of the last ice age (Kapsner et al., 1995; Alley et al., 1997). Self-sustaining feedbacks, including high albedo and input of freshwater, would have augmented cooling and delayed warming around the ice-sheet margins until thousands of years after the summer insolation maximum. As the ice mass diminished, its response time would have likewise decreased, allowing a more rapid reaction to temperature and precipitation changes, perhaps facilitating dynamic ice-margin fluctuations and their accompanying impacts on the adjacent ocean (e.g., Kaufman et al., 1993; Pfeffer et al., 1997).

4.3. *Atmospheric circulation*

In addition to the direct effects of changing boundary conditions and the feedbacks that resulted, the asynchronicity in early Holocene warming was also governed by changes in atmospheric circulation. For example, the spatio-temporal pattern of boreal treeline fluctuations has been attributed to the geometry of the Arctic frontal zone in summer (e.g., Moser and MacDonald, 1990). Similarly, the delayed termination of the HTM in the forest–tundra of northern Quebec compared to sites farther north might suggest that the polar front remained north of the present forest–tundra boundary until 2 ka, when the front moved southward, subjecting these sites to more frequent summertime Arctic air masses (Kerwin et al., submitted). Variations in snow cover, sea ice, and SSTs are influenced by (and themselves influence) the strength and position of prominent surface-pressure features such as the Icelandic and Aleutian lows, and anticyclones and cyclones of the Arctic Basin (Serreze et al., 1993, 2000). During the HTM, the locations of these "centers of action" were probably similar to today because they are basically determined by the major physiographic features and by

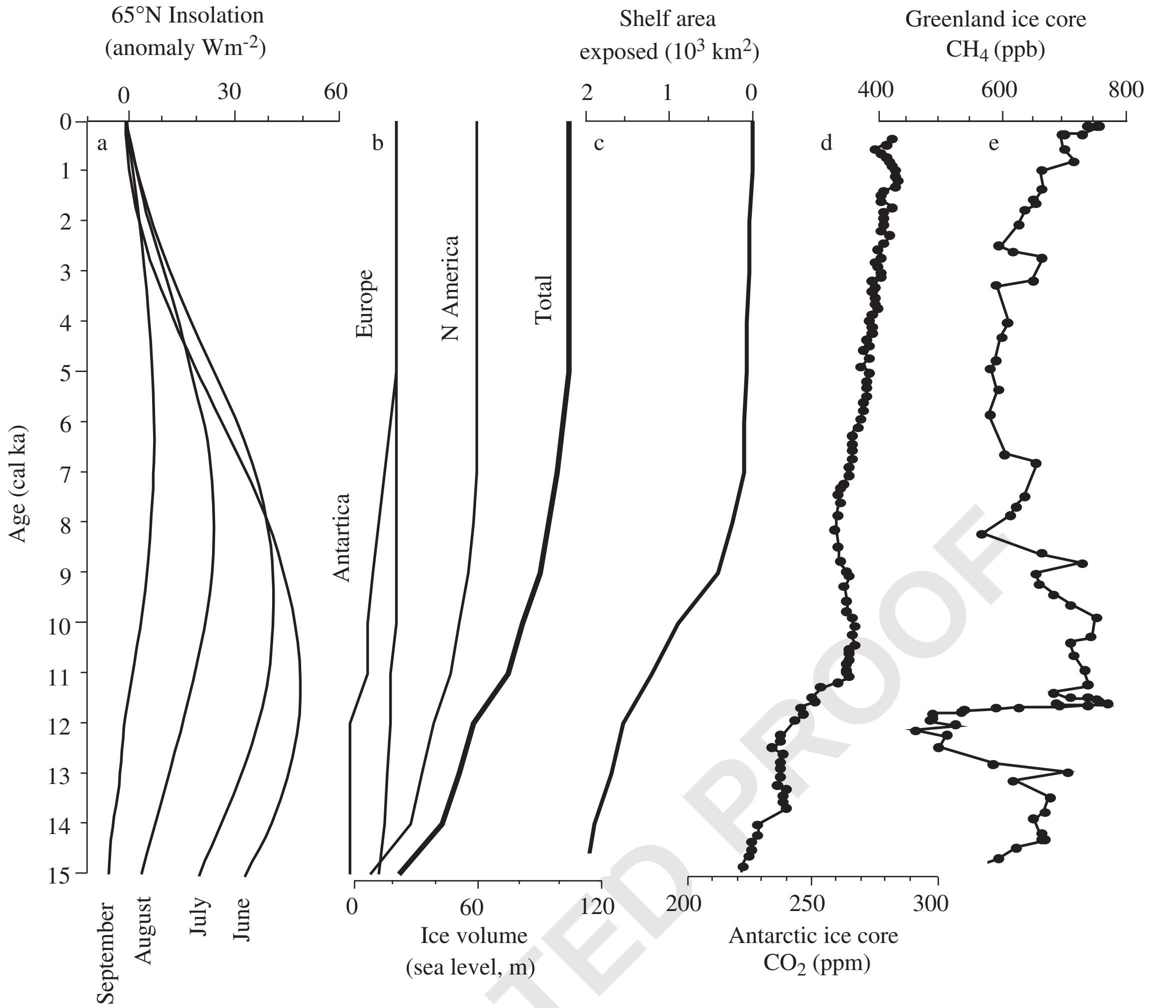

Fig. 9. Global and regional boundary conditions for Holocene climate in the western Arctic. (a) Insolation anomaly for June–September at 65°N (Berger and Loutre, 1991). (b) Approximate ice volume for Antarctica, Europe, and North America, plotted as sea-level equivalent (Peltier, 1994). (c) Approximate extent of continental shelf area exposed as shorelines transgressed the Bering and Chukchi platforms, based on eustatic sea-level record and present-day bathymetry (Manley, 2002). (d) Concentration of atmospheric CO_2 from Antarctica ice cores (Indermühle et al., 2000). (e) Concentration of atmospheric CH_4 from Greenland ice core (GISP2; Brook et al., 1996).

land/ocean contrasts; however, their magnitude (anomalies) and spatial extent varied with time (e.g., Diaz and Andrews, 1982).

Paleoclimate simulations by GCMs show a weakening of the Aleutian low in winter, and strengthening of the eastern Pacific and Bermuda high-pressure systems in summer as the climate evolved following the last glacial maximum (COHMAP, 1988; Bartlein et al., 1998). GCM simulations for the early Holocene suggest that the remnant Laurentide Ice Sheet caused spatial variability in the sign and extent of these pressure anomalies (Mitchell et al., 1988; Mitchell, 1990). At 6 ka, GCM simulations indicate positive pressure anomalies over the North Pacific and negative pressure anomalies over the Arctic Ocean (e.g., Hewitt and Mitchell, 1996; Lorenz et al., 1996). In the North Atlantic region, higher-than-present SSTs further enhanced summer warming at that time (Kerwin et al., 1999).

The spatial pattern of warming observed during the last five decades (e.g., Serreze et al., 2000) resembles the pattern of early Holocene warmth, suggesting that similarities between the two warming phenomena might exist. A growing body of evidence links this pattern of warming and related environmental changes with the Arctic Oscillation (AO), a fundamental mode of Northern Hemisphere atmospheric variability (e.g., Thompson and Wallace, 1998). The high-index state of the AO is characterized by decreased sea-level pressure centered over the pole, and enhanced surface westerly winds that cool northeast North America. Cyclonic circulation in the Arctic Ocean is strengthened, forcing freshwater and sea ice through Fram Strait and the Canadian Archipelago, and lowering surface temperatures over the

Labrador Sea. The high index of the AO is associated with increased surface pressure over the northeast Pacific Ocean, resulting in increased temperatures in the subarctic west of Hudson Bay.

Two differences emerge between the recent warming pattern associated with the AO index and the pattern reconstructed by our paleodata. First, in its high-index state, the AO suggests a negative temperature anomaly in Alaska, whereas the paleodata indicate warming during peak summer insolation. The same issue concerns the instrumental data: warming has occurred in Alaska as the AO indexed has increased. Part of this mismatch might be explained by the strongly heterogeneous response of surface climate in Beringia to even small shifts in the strength or position of circulation patterns in the North Pacific (Mock et al., 1998; Edwards et al., 2001), but this mechanism cannot account for continental-scale patterns. Second, the high-index state of the AO is associated with a weakening of the Beaufort High and a strengthening of cyclonic circulation of surface currents in the Arctic Ocean. The distribution of driftwood in the Canadian Archipelago, however, indicates that the Beaufort Gyre may have been strengthened or shifted westward during the early Holocene (Dyke and Savelle, 2000).

The AO is known to fluctuate as an intrinsic mode of atmospheric variability on relatively short timescales (daily to interannual), and it is detectable in proxy data at multi-centennial timescales (Rimbu et al., 2001; Luterbacher et al., 2002). A mechanistic (as opposed to purely correlative) linkage with the much lower-frequency climate variability represented by early Holocene warmth is difficult to develop, and unlikely to represent an intrinsic mode of atmospheric variability alone. Millennial-scale changes are more easily ascribed to changes in thermohaline circulation, variations in solar output, or to climate feedbacks, none of which would necessarily be expected to result in an AO-like pattern. The self-sustaining properties of the remnant ice sheet in northeast North America and the geographic and oceanographic predisposition of that region to glaciation afford a reasonable explanation for the delayed warmth during the early Holocene. Nonetheless, current understanding of the physical mechanisms controlling the AO suggests that its increasing trend late in the 20th century might be ascribed to radiative forcing from increased atmospheric CO_2 (Moritz et al., 2002). An AO response to solar forcing on millennial timescales is also suggested from some paleodata compilations and modeling results (Shindell et al., 2001; Noren et al., 2002; Rimbu et al., 2003). If so, then it is reasonable to infer that forcing by summer insolation during the early Holocene may have been accompanied by an increased tendency for the AO index to remain elevated. Other climate modes that feature recurring atmospheric circulation anomaly patterns, like ENSO, have distinctive surface-climate responses in the Arctic (e.g., Hurrell, 1996) that could also have promoted additional spatial variability during the HTM.

5. Conclusion

The HTM in the western Arctic was forced primarily by insolation changes governed by orbital variations that scaled with latitude. Despite the symmetrical forcing, the HTM occurred earlier in Alaska and northwest Canada, beginning ca. 11 ka, than in the Hudson Bay region, where the HTM was delayed until after the final melting of the Laurentide Ice Sheet, ca. 7 ka. The HTM in regions strongly influenced by the North Atlantic and Arctic Oceans (Canadian Arctic Islands, Greenland, and Iceland) tended to occur ca. 9 ka. The pronounced spatial and temporal asymmetry in the response to symmetrical forcing underscores the roles of land-cover feedbacks and coupled atmospheric–oceanic dynamics, especially the northward penetration of relatively warm Atlantic Water, as modulators of climatic change in the western Arctic. The lingering ice sheets and their interaction with fluctuating, meridionally oriented ocean currents in the North Atlantic sector resulted in a fundamentally different response compared with the Pacific sector, where the circulation regime is more zonal.

The timing of the HTM varied spatially, but the increase in temperature relative to present was about the same around the western Arctic. At the 16 terrestrial sites where quantitative estimates have been reported, temperatures (mainly summer estimates) were 1.6±0.8°C higher during the HTM than present (approximately the average 20th century). Although the data are sparse, warming in northeast North America appears to have been similar in magnitude to the eastern Beringian sector, relative to modern conditions, even though warming in the northeast took place significantly later in the precessional cycle, when insolation forcing was diminished. Warming in the northeast was augmented by a stronger-than-present northward flow of warm Atlantic Water at that time.

The delayed warming in northeastern North America was associated with the cooling effect of the residual Laurentide Ice Sheet. The self-sustaining feedbacks of the lingering ice and its interaction with ocean circulation is the leading candidate for the overall asymmetric response exhibited by the paleodata. We cannot discern, however, the extent to which the delayed warming in northeastern North America might have been a response to, rather than the cause of, the inherent asymmetry of ocean and atmospheric circulation, which favors glacial conditions in the northwestern North Atlantic over other locations at the same latitude. Spatially varying amplification of the direct effects of insolation forcing also played a role in modulating the spatio-temporal pattern of warming. Regardless of the governing mechanism, the longitudinally asymmetric pattern of warming during the early Holocene exemplifies the contrasting response of the Pacific and Atlantic sectors to symmetrical forcing. This AO-like pattern might represent a preferred mode of variation in the Arctic that could recur in the future. Unlike early Holocene warming, however, future warming will not be counterbalanced by the cooling effects of a residual, decaying North American ice sheet.

6. Uncited references

Bourgeois, 2000; Detterman, 1970; Edwards et al., 2003; Gajewski et al., 1995; Mott, 1978; Mysak and Power, 1992; Richard, 1977; Short et al., 1994.

Acknowledgements

The PARCS-HTM Working Group meeting at the National Center for Atmospheric Research in Boulder, CO was supported by the US National Science Foundation Arctic System Science Program. The participation of the PARCS Data Manager (M. Duvall) and Science Management Officer (L. Coats) was funded through grant NSF-OPP-0218785. Reviews by A. Werner and an anonymous referee improved the paper.

Appendix A. PARCS-HTM Working Group members and workshop participants, Boulder, CO, November, 2002

Ager, Tom, US Geological Survey, Denver, CO, USA, tager@usgs.gov

Anderson, N. John, Geological Survey of Denmark and Greenland, Copenhagen, Denmark, nja@geus.dk

Anderson, Lesleigh, Department of Geosciences, University of Massachusetts, Amherst, USA, land@geo.umass.edu

Anderson, Patricia, Quaternary Research Center, University of Washington, Seattle, USA, pata@u.washington.edu

Andreev, Andrei, Alfred Wegener Institute for Polar and Marine Research, Germany, aandreev@awi-potsdam.de

Andrews, John, Institute of Arctic and Alpine Research, University of Colorado, Boulder, USA, john.t.andrews@colorado.edu

Axford, Yarrow, Institute of Arctic and Alpine Research, University of Colorado, Boulder USA, yarrow.axford@colorado.edu

Bartlein, Pat, Department of Geography, University of Oregon, Eugene, USA, bartlein@oregon.uoregon.edu

Black, Jessica, Institute of Arctic and Alpine Research, University of Colorado, Boulder, USA, jblack@boulder.colorado.edu

Brubaker, Linda, College of Forest Resources, University of Washington, Seattle, USA, lbru@u.washington.edu

Calkin, Parker, Institute of Arctic and Alpine Research, University of Colorado, Boulder, USA, parker.calkin@colorado.edu

Coats, Larry, Department of Geology, Northern Arizona University, Flagstaff, USA, larry.coats@nau.edu

Cwynar, Les, Department of Biology, University of New Brunswick, Fredericton, Canada, cwynar@unb.ca

Douglas, Marianne, Department of Geology, University of Toronto, Ontario, Canada, msvd@geology.utoronto.ca

Duvall, Mathieu, Department of Geology, Bates College, Lewiston, ME, USA, mduvall@bates.edu

Dyke, Art, Geological Survey of Canada, Ottawa, Ont., Canada, adyke@nrcan.gc.ca

Edwards, Mary, Institute of Geography, University of Trondheim, Norway, mary.edwards@svt.ntnu.no

Edwards, Thomas, Department of Earth Sciences, University of Waterloo, Ontario, Canada, twdedwar@uwaterloo.ca

Eisner, Wendy, Department of Geography, University of Cincinnati, Ohio, USA, wendy.eisner@uc.edu

Forman, Steve, Department of Earth and Environmental Sciences, University of Illinois, Chicago, USA, slf@uic.edu

Gajewski, Konrad, Department of Geography, University of Ottawa, Ontario, Canada, gajewski@aix1.uottawa.ca

Geirsdóttir, Áslaug, Department of Geosciences, University of Iceland, Reykjavik, Iceland, age@rhi.hi.is

Hu, Feng Sheng, Department of Plant Biology, University of Illinois, Urbana, USA, fshu@life.uiuc.edu

Jennings, Anne, Institute of Arctic and Alpine Research, University of Colorado, Boulder, USA, jenninga@spot.colorado.edu

Kaplan, Michael, School of Geosciences, University of Edinburgh, UK, mkaplan@geo.ed.ac.uk

Kaufman, Darrell, Department of Geology, Northern Arizona University, Flagstaff, USA, darrell.kaufman@nau.edu

Kerwin, Michael, Department of Geography, University of Denver, Colorado, USA, mkerwin@du.edu

Koç, Nolân, Norwegian Polar Institute, Tromsø, Norway, nalan.koc@npolar.no

Korhola, Atte, Department of Ecology and Systematics, University of Helsinki, Finland, atte.korhola@helsinki.fi

Levis, Samuel, National Center for Atmospheric Research, Boulder, CO, USA, slevis@cgd.ucar.edu

Lozhkin, Anatoly, Northeast Interdisciplinary Science Research Institute, Russian Academy of Sciences, Magadan, Russia, lozhkin@neisri.magadan.ru

Lubinski, David, Institute of Arctic and Alpine Research, University of Colorado, Boulder, USA, david.lubinski@colorado.edu

Lynch, Manda, Cooperative Institute for Research in Evironmnetal Sciences, Universtiy of Colorado, Boulder, USA, manda@cires.colorado.edu

MacDonald, Glen, Department of Geography, University of California, Los Angelas, USA, macdonal@geog.ucla.edu

Mangerud, Jan, Department of Earth Science, University of Bergen, Norway, jan.mangerud@geol.uib.no

Manley, William, Institute of Arctic and Alpine Research, University of Colorado, Boulder, USA, manleyw@ucsu.colorado.edu

Miller, Gifford, Institute of Arctic and Alpine Research, University of Colorado, Boulder, USA, gmiller@colorado.edu

Mock, Cary, Department of Geography, University of South Carolina, Columbia, USA, mockcj@gwm.sc.edu

Oswald, Wyatt, Quaternary Research Center, University of Washington, Seattle, USA, woswald@u.washington.edu

Otto-Bliesner, Bette, National Center for Atmospheric Research, Boulder, CO, USA, ottobli@ncar.ucar.edu

Overpeck, Jonathan, Institute for the Study of Planet Earth, University of Arizona, Tucson, USA, jto@u.arizona.edu

Porinchu, David, Department of Geography, California State University, Long Beach, USA, porinchu@ucla.edu

Ruhland, Kathleen, Department of Biology, Queen's University, Kingston, Ont., Canada, 3kmr5@biology.queensu.ca

Smol, John, Department of Biology, Queen's University, Kingston, Ont., Canada, smolj@biology.queensu.ca

Spear, Ray, Department of Biology, State Univeristy of New York, Geneseo, USA, spear@uno.cc.geneseo.edu

Steig, Eric, Quaternary Research Center, University of Washington, Seattle, USA, steig@geophys.washington.edu

Vartanyan, Seregey, Wrangel Island State Preserve, Magadan Region, Russia, diana@ds3902.spb.edu

Velichko, Andrei, Paleoclimate Laboratory, Russian Academy of Sciences, Moscow, Russia, paleo@online.ru

Wolfe, Brent, Department of Geography and Environmental Studies, Wilfrid Laurier University, Waterloo, Ont., Canada, bwolfe@wlu.ca

References

Abbott, M.B., Finney, B.P., Edwards, M.E., Kelts, K.R., 2000. Lake-level reconstruction and paleohydrology of Birch Lake, central Alaska, based on seismic reflection profiles and core transects. Quaternary Research 53, 154–166.

Ager, T.A., 1982. Vegetational history of western Alaska during the Wisconsin glacial interval and the Holocene. In: Hopkins, D.M., Matthews Jr., J.V., Schweger, C.E., Young, S.B. (Eds.), Paleoecology of Beringia. Academic Press, New York, pp. 75–93.

Ager, T.A., 1983. Holocene vegetational history of Alaska. In: Wright Jr., H.E. (Ed.), Late Quaternary Environments of the United States. The Holocene, Vol. 2. University of Minnesota Press, Minneapolis, MN, pp. 128–141.

Ager, T.A., 1989. History of late Pleistocene and Holocene vegetation in the Copper River basin, south-central Alaska. In: Carter, L.D., Hamilton, T.D., Galloway, J.P. (Eds.), Late Cenozoic History of the Interior Basins of Alaska and the Yukon. US Geological Survey Circular 1026, 89–92.

Ager, T.A., 2003. Late Quaternary vegetation and climate history of the central Bering land bridge from St. Michael Island, western Alaska. Quaternary Research 60, 19–32.

Alley, R.B., Mayewski, P.A., Sowers, T., Stuiver, M., Taylor, K.C., Clark, P.U., 1997. Holocene climatic instability: a prominent, widespread event 8200 years ago. Geology 25, 483–486.

Anderson, N.J., Grauert, M., McGowan, S., in press. Holocene paleolimnology of Greenland, the North Atlantic Islands. In: Pienitz, R., Douglas, M.S.V., Smol, J.P. (Eds.), Long-Term Environmental Change in Arctic and Antarctic Lakes. Kluwer, Dordrecht.

Anderson, P.M., 1988. Late Quaternary pollen records from the Noatak and Kobuk River drainages, northwestern Alaska. Quaternary Research 29, 263–267.

Anderson, P.M., Lozhkin, A.V., Brubaker, L.B., 2002a. Implications of a 24,000-yr palynological record for a Younger Dryas cooling and for boreal forest development in northeastern Siberia. Quaternary Research 57, 325–333.

Anderson, P.M., Kotov, A.N., Lozhkin, A.V., Trumpe, M.A., 2002b. Palynological and radiocarbon data from late Quaternary deposits of Chukotka. In: Simakov, K.V. (Ed.), Late Quaternary Vegetation and Climate of Siberia and the Russian Far East (Palynological and Radiocarbon Database). North East Science Center Far East Branch, Russian Academy of Sciences, Magadan, pp. 35–79.

Andrews, J.T., 1972. Recent and fossil growth rates of marine bivalves, Canadian Arctic, and 1ate-Quaternary Arctic marine environments. Palaeogeography, Palaeoclimatology, Palaeoecology 11, 157–176.

Andrews, J.T., 1973. The Wisconsin Laurentide Ice Sheet: dispersal centers, problems of retreat, and climatic implications. Arctic and Alpine Research 5, 185–199.

Andrews, J.T., 1987. The late Wisconsin glaciation and deglaciation of the Laurentide Ice Sheet. In: Ruddiman, W.F., Wright Jr., H.E. (Eds.), North America and Adjacent Oceans During the Last Deglaciation. The Geology of North America, Vol. K-3. Geological Society of America, Boulder, CO, pp. 13–37.

Andrews, J.T., 1989. Quaternary geology of the northeastern Canadian Shield. In: Fulton, R.J. (Ed.), Quaternary Geology of Canada and Greenland. Geological Society of America, Boulder, CO, pp. 276–301.

Andrews, J.T., Giraudeau, J., 2003. Multi-proxy records showing significant Holocene environmental variability: the inner N. Iceland Shelf (Húnaflói). Quaternary Science Reviews 22, 175–193.

Andrews, J.T., Erlenkeuser, H., Evans, L., Briggs, W., Jull, A.J.T., 1991. Meltwater and deglaciation SE Baffin Shelf (NE margin Laurentide Ice Sheet) between 13.5 and 8 ka: from stable O and C data. Paleoceanography 6, 621–637.

Andrews, J.T., Smith, L.M., Preston, R., Cooper, T., Jennings, A.E., 1997. Spatial and temporal patterns of iceberg rafting (IRD) along the East Greenland margin, ca. 68 N, over the last 14 cal ka. Journal of Quaternary Science 12, 1–13.

Andrews, J.T., Keigwin, L., Hall, F., Jennings, A.E., 1999. Abrupt deglaciation events and Holocene paleoceanography from high resolution cores, Cartwright Saddle, Labrador Shelf, Canada. Journal of Quaternary Science 14, 383–397.

Andrews, J.T., Helgadottir, G., Geirsdottir, A., Jennings, A.E., 2001. Multicentury-scale records of carbonate (hydrographic?) variability on the North Iceland margin over the last 5000 yrs. Quaternary Research 56, 199–206.

Andrews, J., Geirsdóttir, A., Hardadóttir, J., Principato, S., Grönvold, K., Kristjansdóttir, G., Helgadóttir, G., Drexler, J., Sveinbjörnsdóttir, A., 2002. Distribution, sediment magnetism and geochemistry of the Saksunarvatn (10180 ± 60 cal yr BP) tephra in marine, lake, and terrestrial sediments, northwest Iceland. Journal of Quaternary Science 17, 731–745.

Andrews, J.T., Hardadottir, J., Stoner, J.S., Mann, M.E., Kristjansdottir, G.B., Koc, N., 2003. Decadal to millennial-scale periodicities in North Iceland shelf sediments over the last 12,000 cal yrs: long-term North Atlantic oceanographic variability and solar forcing. Earth and Planetary Science Letters 210, 453–465.

Barber, V.A., Finney, B.P., 2000. Late Quaternary paleoclimatic reconstructions for interior Alaska based on paleolake-level data and hydrologic models. Journal of Paleolimnology 24, 29–41.

Barber, D.C., Dyke, A., Hillaire-Marcel, C., Jennings, A.E., Andrews, J.T., Kerwin, M.W., Bilodeau, G., McNeely, R., Southon, J., Moorehead, M.D., Gagnon, J.-M., 1999. Forcing of the cold event of 8200 years ago by catastrophic drainage of Laurentide lakes. Nature 400, 344–348.

Bartlein, P.J., Anderson, P.M., Edwards, M.E., McDowell, P.F., 1992. A framework for interpreting paleoclimatic variations in eastern Beringia. Quaternary International 10–12, 73–83.

Bennike, O., 2000. Palaeoecological studies of Holocene lake sediments from west Greenland. Palaeogeography, Palaeoclimatology, Palaeoecology 155, 285–304.

Bartlein, P.J., Anderson, K.H., Anderson, P.M., Edwards, M.E., Mock, C.J., Thompson, R.S., Webb, R.S., Whitlock, C., 1998. Paleoclimate simulations for North America over the past 21,000 years: features of the simulated climate and comparisons with the paleoenvironmental data. Quaternary Science Reviews 17, 549–585.

Bennike, O., Weidick, A., 2001. Late Quaternary history around Nioghalvfjerdsfjorden and Jøkelbugten, North-East Greenland. Boreas 30, 205–227.

Berger, A., Loutre, M.F., 1991. Insolation values for the climate of the last 10 million of years. Quaternary Science Reviews 10, 297–317.

Bigelow, N.H., Edwards, M.E., 2001. A 14,000 yr paleoenvironmental record from Windmill Lake, Central Alaska: lateglacial and Holocene vegetation in the Alaska range. Quaternary Science Reviews 20, 203–215.

Birks, H.J.B., Birks, H.H., 1980. Quaternary Paleoecology. University Park Press, Baltimore, MD, 289pp.

Birks, C.J.A., Koç, N., 2002. A high-resolution diatom record of Late-Quaternary sea-surface temperatures and oceanographic conditions from the eastern Norwegian Sea. Boreas 31, 323–344.

Blunier, T., Chappellaz, J., Schwander, J., Stauffer, B., Raynaud, D., 1995. Variations in atmospheric methane concentration during the Holocene epoch. Nature 374, 46–49.

Bond, G., Kromer, B., Beer, J., Muscheler, R., Evans, M., Showers, W., Hoffmann, S., Lotti-Bond, R., Hajdas, I., Bonani, G., 2001. Persistent solar influence on North Atlantic climate during the Holocene. Science 294, 2130–2136.

Bourgeois, J.C., 2000. Seasonal and interannual pollen variability in snow layers of Arctic ice caps. Review of Palaeobotany and Palynology 108, 17–36.

Bourgeois, J.C., Koerner, R.M., Gajewski, K., Fisher, D.A., 2000. A Holocene ice-core pollen record from Ellesmere Island, Nunavut, Canada. Quaternary Research 54, 275–283.

Bourgeois, J.C., Gajewski, K., Koerner, R., 2001. Spatial patterns of pollen deposition in Arctic snow. Journal of Geophysical Research 106, 5255–5565.

Brassard, G.R., Blake, W.J., 1978. An extensive subfossil deposit of the Arctic moss Aplodon wormskioldii. Canadian Journal of Botany 56, 1852–1859.

Briffa, K.R., Jones, P.D., Schwiengruber, F.H., Osborn, T.J., 1998. Influence of volcanic eruptions on Northern Hemisphere summer temperatures over the past 600 years. Nature 393, 450–455.

Broecker, W.S., Denton, G.H., 1989. The role of ocean–atmosphere reorganizations in glacial cycles. Geochimica et Cosmochimica Acta 53, 2465–2501.

Brook, E.J., Sowers, T., Orchardo, J., 1996. Rapid variations in atmospheric methane concentration during the past 110,000 years. Science 273, 1087–1091.

Brubaker, L., Garfinkel, H., Edwards, M., 1983. A late Wisconsin and Holocene vegetation history from the central Brooks Range: implications for Alaskan paleoecology. Quaternary Research 20, 194–214.

Brubaker, L.B., Anderson, P.M., Hu, F.S., 2001. Vegetation ecotone dynamics in southwest Alaska during the late Quaternary. Quaternary Science Reviews 20, 175–188.

Bryson, R.A., Irving, W.N., Larsen, J.A., 1965. Radiocarbon and soil evidence of former forest in the southern Canadian tundra. Science 147, 46–48.

Burn, C.R., 1997. Cryostratigraphy, paleogeography, and climate change during the early Holocene warm interval, western Arctic coast, Canada. Canadian Journal of Earth Sciences 34, 912–925.

Burn, C.R., Michel, F.A., Smith, M.W., 1986. Stratigraphic, isotopic, and mineralogical evidence for an early Holocene thaw unconformity at Mayo, Yukon Territory. Canadian Journal of Earth Sciences 23, 79–803.

Calkin, P.E., 1988. Holocene glaciation of Alaska (and adjoining Yukon Territory, Canada). Quaternary Science Reviews 7, 159–184.

CAPE Project Members, 2001. Holocene paleoclimate data from the Arctic: testing models of global climate change. Quaternary Science Reviews 20, 1275–1287.

Caseldine, C., Geirsdóttir, Á., Langdon, P., 2003. Efstadalsvatn—a multi-proxy study of a Holocene lacustrine sequence from NW Iceland. Journal of Paleolimnology 30, 55–73.

Castaneda, I.S., Smith, L.M., Kristjansdottir, G.B., Andrews, J.T., 2003. Holocene δ^{18}O records of paleoceanographic and climatic variability from the Northern Iceland continental shelf.

Chamberlin, T.C., 1899. An attempt to frame a working hypothesis of the cause of glacial periods on an atmospheric basis. Journal of Geology 7, 545–584, 751–787, 667–685.

Chapin III, F.S., McGuire, A.D., Randerson, J., Pielke Sr., R., Baldocchi, D., Hobbie, S.E., Roulet, N., Eugster, W., Kaisischke, E., Rastetter, E.B., Zimov, S.A., Running, S.W., 2000. Arctic and boreal ecosystems of western North America as components of the climate system. Global Change Biology 6, 211–223.

Christiansen, H., Bennike, O., Böcher, J., Elberling, B., Humlum, O., Jakobsen, B., 2002. Holocene environmental reconstruction from deltaic deposits in northeast Greenland. Journal of Quaternary Science 17, 145–160.

Clark, P.U., Pisias, N.G., Stocker, T.F., Weaver, A.J., 2002. The role of thermohaline circulation in abrupt climate change. Nature 415, 863–869.

COHMAP Members, 1988. Climatic changes of the last 18,000 years: observations and model simulations. Science 241, 1043–1052.

Colinvaux, P.A., 1967a. A long pollen record from St. Lawrence Island, Bering Sea, Alaska. Palaeogeography, Palaeoclimatology, Palaeoecology 3, 29–43.

Colinvaux, P.A., 1967b. Bering land bridge: evidence of spruce in late Wisconsin times. Science 156, 380–383.

Colinvaux, P.A., 1981. Historical ecology in Beringia: the south land bridge coast at St. Paul Island. Quaternary Research 16, 18–36.

Cremer, H., Melles, M., Wagner, B., 2001a. Holocene climate changes reflected in a diatom succession from Basaltsø, East Greenland. Canadian Journal of Botany 79, 649–656.

Cremer, H., Wagner, B., Melles, M., Hubberten, H.W., 2001b. The postglacial environmental development of Raffles Sø, East Greenland: inferences from a 10,000 year diatom record. Journal of Paleolimnology 26, 67–87.

Crossen, K.J., Pasch, A.D., Barker, M.H., 2002. Bering glacier retreat phase: discoveries of overrun fiords and forests. Geological Society of America Abstracts and Programs 34 (6), 477.

Crucifix, M., Loutre, M.-F., Tulkens, P., Fichefet, T., Berger, A., 2002. Climate evolution during the Holocene: a study with an earth system model of intermediate complexity. Climate Dynamics 19, 43–60.

Cubasch, U., Crowley, T.J., Voss, R., Hegerl, G.C., Waszkewitz, J., 1997. Simulation of the influence of solar radiation variations on the global climate with an ocean–atmosphere general circulation model. Climate Dynamics 13, 757–767.

Cuffey, K., Clow, G., 1997. Temperature, accumulation, and ice sheet elevation in central Greenland through the last deglacial transition. Journal of Geophysical Research 102, 26383–26396.

Cuffey, K.M., Clow, G.D., Alley, R.B., Stuiver, M., Waddington, E.D., Saltus, .R.W., 1995. Large Arctic temperature change at the Wisconsin–Holocene transition. Science 270, 455–458.

Cwynar, L.C., 1982. A Late-Quaternary vegetation history from Hanging Lake, northern Yukon. Ecological Monographs 52, 1–24.

Cwynar, L.C., 1988. Late Quaternary vegetation history of Kettlehole Pond, southwestern Yukon. Canadian Journal of Forest Research 18, 1270–1279.

Cwynar, L.C., Spear, R.W., 1991. Reversion of forest to tundra in the central Yukon. Ecology 72, 202–212.

Cwynar, L.C., Spear, R.W., 1995. Paleovegetation and paleoclimatic changes in the Yukon at 6 ka BP. Geographie Physique et Quaternaire 49, 29–35.

Dahl-Jensen, D., Mosegaard, K., Gundestrup, N., Clow, G., Johnsen, S., Hansen, A., Balling, N., 1998. Past temperatures directly from the Greenland Ice Sheet. Science 282, 268–271.

Dansgaard, W., Johnsen, S., Clausen, H., Langway Jr., C.C., 1971. Climatic record revealed by the Camp Century ice core. In: Turekian, K.K. (Ed.), The Late Cenozoic Glacial Ages. Yale University Press, New Haven, CT, pp. 37–56.

Detterman, R.L., 1970. Early Holocene warm interval in northern Alaska. Arctic 23, 130–131.

Diaz, H.F., Andrews, J.T., 1982. Analysis of the spatial pattern of July temperature departures (1943–1972) over Canada and estimates of the 700 mb mid-summer circulation during middle and late Holocene. Journal of Climatology 2, 251–265.

Dyke, A.S., 1999. Last glacial maximum and deglaciation of Devon Island, Arctic Canada: support for an Innuitian ice sheet. Quaternary Science Reviews 18, 393–420.

Dyke, A.S., Peltier, W.R., 2000. Forms, response times and variability of relative sea-level curves, glaciated North America. Geomorphology 32, 315–333.

Dyke, A.S., Prest, V.K., 1987a. Late Wisconsinan and Holocene history of the Laurentide Ice Sheet. Geographie Physique et Quaternaire 41, 237–263.

Dyke, A.S., Prest, V.K., 1987b. Paleogeography of northern North America, 18000–5000 years ago. Geological Survey of Canada.

Dyke, A.S., Savelle, J.M., 2000. Holocene driftwood incursion to southwestern Victoria Island, Canadian Arctic Archipelago, and its significance to paleoceanography and archaeology. Quaternary Research 54, 113–120.

Dyke, A.S., Savelle, J.M., 2001. Holocene history of the Bering Sea bowhead whale (*Balaena mysticetus*) in its Beaufort Sea summer grounds off southwestern Victoria Island, western Canadian Arctic. Quaternary Research 55, 371–379.

Dyke, A.S., Hooper, J., Savelle, J.M., 1996a. A history of sea ice in the Canadian Arctic Archipelago based on postglacial remains of the bowhead whale (*Balaena mysticetus*). Arctic 49, 235–255.

Dyke, A.S., Dale, J.E., McNeely, R.N., 1996b. Marine molluscs as indicators of environmental change in glaciated North America and Greenland during the last 18000 years. Géographie Physique et Quaternaire 50, 125–184.

Dyke, A.S., Hooper, J., Harington, C.R., Savelle, J.M., 1999. The Late Wisconsinan and Holocene record of walrus (*Odobenus rosmarus*) from North America: a review with new data from Arctic and Atlantic Canada. Arctic 52, 160–181.

Dyke, A.S., Andrews, J.T., Clark, P.U., England, J.H., Miller, G.H., Shaw, J., Veillette, J.J., 2002. The Laurentide and Innuitian ice sheets during the last glacial maximum. Quaternary Science Reviews 21, 9–31.

Edwards, M.E., Barker, E.D., 1994. Climate and vegetation in northeastern Alaska 18,000 yr BP–present. Paleogeography, Paleoclimatology, Paleoecology 109, 127–135.

Edwards, M.E., Brigham-Grette, J., 1990. Climatic change and thaw-lake formation in Alaska. 11th Biennial Meeting of the American Quaternary Association, Waterloo, Ont., p. 17.

Edwards, M.E., Dunwiddie, P.W., 1985. Dendrochronological and palynological observations on *Populus balsamifera* in northern Alaska, USA. Arctic and Alpine Research 17, 271–278.

Edwards, M.E., Anderson, P.M., Garfinkel, H.L., Brubaker, L.B., 1985. Late Wisconsin and Holocene vegetation history of the upper Koyukuk region, Brooks Range, Alaska. Canadian Journal of Botany 63, 616–646.

Edwards, T.W.D., Wolfe, B.B., MacDonald, G.M., 1996. Influence of changing atmospheric circulation on precipitation δ^{18}O-temperature relations in Canada during the Holocene. Quaternary Research 46, 211–218.

Edwards, M.E., Mock, C.J., Finney, B.P., Barber, V., Bartlein, P.J., 2001. Potential analogues for paleoclimatic variations in eastern interior Alaska for the past 14,000 years: atmospheric-circulation controls of regional temperature and moisture responses. Quaternary Science Reviews 20, 189–202.

Edwards, M.E., Anderson, P., Brubaker, L., 2003. Results and paleoclimate implications of 35 years of paleoecological research n Alaska. In: Gillespie, A., Porter, S., Atwater, B. (Eds.), The Quaternary Period in the United States. Elsevier Press, Amsterdam, in press.

Eirîksson, J., Knudsen, K.L., Haflidason, H., Henriksen, P., 2000. Late-glacial and Holocene paleoceanography of the North Iceland Shelf. Journal of Quaternary Science 15, 23–42.

Eisner, W.R., 1991. Palynological analysis of a peat core from Imnavait Creek, the North Slope, Alaska. Arctic 44, 279–282.

Eisner, W.R., Peterson, K.M., 1998. High-resolution pollen analysis of tundra polygons from the North Slope of Alaska. Journal of Geophysical Research 103, 28929–28937.

Eisner, W.R., Törnqvist, T.E., Koster, E.A., Bennike, O., Vanleeuwen, J.F.N., 1995. Paleoecological studies of a Holocene lacustrine record from the Kangerlussuaq (Sondre Stromfjord) region of west Greenland. Quaternary Research 43, 55–66.

Eugster, W., Rouse, W.R., Pielke Sr., R.A., McFadden, J.P., Baldocchi, D.D., Kittel, T.G.F., Chapin III, F.S., Liston, G.E., Vidale, P.L., Vaganov, E., Chambers, S., 2000. Land-atmosphere energy exchange in Arctic tundra and boreal forest: available data and feedbacks to climate. Global Change Biology 6 (Suppl. 1), 84–115.

Fisher, D.A., 1992. Possible ice-core evidence for a fresh meltwater cap over the Atlantic Ocean in the early Holocene. In: Bard, E. (Ed.), The Last Deglaciation: Absolute and Radiocarbon Chronologies, NATO Advanced Workshop ASI Series, Vol. 12. Springer, Berlin.

Fisher, D.A., Koerner, R.M., 2003. Holocene ice core climate history, a multi-variable approach. In: Global Change in the Holocene, Arnold, London, in press.

Fisher, D.A., Koerner, R.M., Reeh, N., 1995. Holocene climatic records from Agassiz Ice Cap, Ellesmere Island, NWT, Canada. The Holocene 5, 19–24.

Fisher, D.A., Koerner, R.M., Bourgeois, J.C., Zielinski, G., Wake, C., Hammer, C.U., Clausen, H.B., Gundestrup, N., Johnsen, S., Goto-Azuma, K., Hondoh, T., Blake, E., Gerasimoff, M., 1998. Penny Ice Cap cores, Baffin Island, Canada, and the Wisconsinan Foxe Dome connection: two states of Hudson Bay ice cover. Science 279, 692–695.

Fisher, T.G., Smith, D.G., Andrews, J.T., 2002. Preboreal oscillation caused by a glacial Lake Agassiz flood. Quaternary Science Reviews 21, 873–878.

Fisher, D.A., et al., in press. The effects of flow-line length evolution on the chemistry-δ^{18}O profiles from the Penny Ice Cap, Baffin Island, Canada. Annals of Glaciology 35.

Foley, J.A., Kutzback, J.E., Coe, M.T., Levis, S., 1994. Feedbacks between climate and boreal forests during the Holocene epoch. Nature 371, 52–54.

Folland, C.K., Karl, T.R., Christy, J.R., Clarke, R.A., Gruza, G.V., Jouzel, J., Mann, M.E., Oerlemans, J., Salinger, M.J., Wang, S.-W., 2001. Observed climate variability and change. In: Houghton, J.T., Griggs, D.J., Nogner, M., van der Linden, P.J., Dai, X., Maskell, K., Johnson, C.A. (Eds.), Climatic Change 2001: the Scientific Basis, Contribution of Working Group I to the Third Assessment Report of the Intergovernmental Panel on Climate Change. Cambridge University Press, Cambridge, UK, pp. 99–182.

Fredskild, B., 1973. Studies in the vegetational history of Greenland. Meddelelser om Grønland 198, 1–245.

Fredskild, B., 1983. The Holocene vegetational development of the Godthåbsfjord area, west Greenland. Meddelelser om Grønland. Bioscience 10, 2–28.

Fredskild, B., 1984. Holocene palaeo-winds and climatic changes in West Greenland as indicated by long-distance transported and local pollen in lake sediments. In: Mörner, N.-A., Karlén, W. (Eds.), Climatic Changes on a Yearly to Millennial Basis. Reidel Publishing, Dordrecht, pp. 163–171.

Fredskild, B., 1992. The Greenland limnophytes—their present distribution and Holocene history. Acta Botony Fennica 144, 93–113.

Funder, S. (co-ordinator), 1989. Quaternary geology of the ice-free areas and adjacent shelves of Greenland. In: Fulton, R.J. (Ed.), Quaternary Geology of Canada and Greenland (Geology of Canada). Geological Society of America, Boulder, CO, pp. 741–792.

Funder, S., Weidick, A., 1991. Holocene boreal molluscs in Greenland: paleoceanographic implications. Palaeogeography, Palaeoclimatology, Palaeoecology 85, 123–135.

Gajewski, K., 1995. Modern and Holocene pollen assemblages from some small Arctic lakes on Somerset Island, NWT, Canada. Quaternary Research 44, 228–236.

Gajewski, K., Frappier, M., 2001. A Holocene lacustrine record of environmental change in northeastern Prince of Wales Island, Nunavut, Canada. Boreas 30, 285–289.

Gajewski, K., Garralla, S., 1992. Holocene vegetation histories from three sites in the tundra of northwestern Quebec, Canada. Arctic and Alpine Research 24, 329–336.

Gajewski, K., Payette, S., Ritchie, J.C., 1993. Holocene vegetation history at the boreal forest—shrub tundra transition in northern Quebec. Journal of Ecology 81, 433–443.

Gajewski, K., Garneau, M., Bourgeois, J.C., 1995. Paleoenvironments of the Canadian High Arctic derived from pollen and plant macrofossils: problems and potentials. Quaternary Science Reviews 14, 609–629.

Gajewski, K., Garralla, S., Milot-Roy, V., 1996. Postglacial vegetation at the northern limit of lichen woodland in northwestern Quebec. Géographie Physique et Quaternaire 50, 341–350.

Gajewski, K., Mott, R., Ritchie, J., Hadden, K., 2000. Holocene vegetation history of Banks Island, Northwest Territories, Canada. Canadian Journal of Botany 78, 430–436.

Gajewski, K., Viau, A., Sawada, M., Atkinson, D., Wilson, S., 2001. *Sphagnum* peatland distribution in North America and Eurasia during the past 21,000 years. Global Biogeochemical Cycles 15, 297–310.

Geirsdóttir, Á., Andrews, J.T., Ólafsdóttir, S., Helgadóttir, G., Hardardóttir, J., 2002. A 35 Ka record of iceberg rafting from NW Iceland; following the ice retreat from the shelf to land. Polar Research 21, 291–298.

Gervais, B.R., MacDonald, G.M., 2001. Tree-ring and summer temperature response to volcanic aerosol forcing at the northern tree-line, Kola Peninsula, Russia. The Holocene 11, 499–505.

Gildor, H., Tziperman, E., 2001. A sea ice climate switch mechanism for the 100-kyr glacial cycles. Journal of Geophysical Research 106, 9117–9133.

Giraudeau, G., Cremer, M., Manthe, S., Laberrie, L., Bond, G., 2000. Coccolith evidence for instabilities in surface circulation south of Iceland during Holocene times. Earth and Planetary Science Letters 179, 257–268.

Grootes, P., Stuiver, M., White, J., Johnsen, S., Jouzel, J., 1993. Comparison of oxygen isotope records from the GISP2 and GRIP Greenland ice cores. Nature 366, 552–554.

Hagen, S., 1995. Watermass characteristics and climate in the Nordic Seas during the last 10,200 years. Candidatus Scientiarum, University of Tromso, Norway, 114pp.

Hallsdóttir, M., 1991. Studies in the vegetational history of north Iceland; a radiocarbon-based pollen diagram from Flateyjardalur. Jökull 40, 67–81.

Hallsdóttir, M., 1995. On the pre-settlement history of Icelandic vegetation. Icelandic Agriculture Science 9, 17–29.

Heusser, C.J., Heusser, L.E., Peteet, D.M., 1985. Late-Quaternary climatic change on the American North Pacific coast. Nature 315, 485–487.

Hewitt, C.D., Mitchell, J.F.B., 1996. GCM simulations of the climate of 6 kyr BP: mean changes and changes and interdecadal variability. Journal of Climate 9, 3505–3529.

Hjort, C., Funder, S., 1974. The subfossil occurrence of *Mytilus edulis* L. in central East Greenland. Boreas 3, 23–33.

Hooke, R.L., Clausen, H.B., 1982. Wisconsin and Holocene δ^{18}O variations, Barnes Ice Cap, Canada. Geological Society of American Bulletin 93, 784–789.

Hopkins, D.M., 1972. The paleogeography and climatic history of Beringia during late Cenozoic time. International Journal of Arctic and Nordic Studies 12, 121–150.

Hopkins, D.M., MacNeil, F.S., Leopold, E.B., 1960. The coastal plain at Nome, Alaska: a late Cenozoic type section for the Bering Strait region. 21st International Geologic Congress, Copenhagen, Part 4, pp. 46–57.

Hopkins, D.M., Smith, P.A., Matthews Jr., J.V., 1981. Dated wood from Alaska and the Yukon: implications for forest refugia in Beringia. Quaternary Research 15, 217–249.

Hu, F.S., Brubaker, L.B., Anderson, P.M., 1993. A 12,000 year record of vegetation change and soil development from Wien Lake, central Alaska. Canadian Journal of Botany 71, 1133–1142.

Hu, F.S., Brubaker, L.B., Anderson, P.M., 1996. Boreal ecosystem development in the northwestern Alaska range since 11,000 yr. B.P. Quaternary Research 45, 188–201.

Hu, F.S., Ito, E., Brubaker, L.B., Anderson, P.M., 1998. Ostracode geochemical record of Holocene climatic change and implications for vegetational response in the northwestern Alaska Range. Quaternary Research 49, 86–95.

Hurrell, J.W., 1996. Influence of variations in extratropical wintertime teleconnections on the Northern Hemisphere temperature. Geophysical Research Letters 23, 665–668.

Hutton, M., MacDonald, G.M., Mott, R.J., 1994. Postglacial vegetation history of the Mariana Lake region, Alberta. Canadian Journal of Earth Sciences 31, 418–425.

Hyvärinen, H., 1985. Holocene pollen stratigraphy of Baird Inlet, east-central Ellesmere Island, Arctic Canada. Boreas 14, 19–32.

Indermühle, A., Stocker, T.F., Joos, F., Fisher, H., Smith, H.J., Wahlen, M., Deck, B., Mastroianni, D., Tschumi, J., Blunier, T., Meyer, R., Stauffer, B., 2000. Holocene carbon-cycle dynamics based on CO_2 trapped in ice at Taylor Dome, Antarctica. Nature 398, 121–126.

Jennings, A., Knudsen, K., Hald, M., Hansen, C., Andrews, J., 2002. A mid-Holocene shift in Arctic sea-ice variability on the East Greenland Shelf. The Holocene 12, 49–58.

Jiang, H., Seidenkrantz, M.-S., Knudsen, K.-L., Eiriksson, J., 2002. Late-Holocene summer sea-surface temperatures based on a diatom record from the north Icelandic shelf. The Holocene 12, 137–148.

Johnsen, S., Clausen, H., Dansgaard, W., Fuhrer, K., Gundestrup, N., Hammer, C., Iversen, P., Jouzel, J., Stauffer, B., Steffensen, J., 1992. Irregular glacial interstadials recorded in a new Greenland ice core. Nature 359, 311–313.

Johnsen, S., Dahl-Jensen, D., Gundestrup, N., Steffensen, J., Clausen, H., Miller, H., Masson-Delmotte, V., Sveinbjörnsdottir, A., White, J., 2001. Oxygen isotope and palaeotemperature records from six Greenland ice-core stations: Camp Century, Dye-3, Grip, GISP2, Renland and Northgrip. Journal of Quaternary Science 16, 299–307.

Kaplan, M., Wolfe, A., Miller, G., 2002. Holocene environmental variability in southern Greenland inferred from lake sediments. Quaternary Research 58, 149–159.

Kapsner, W.R., Alley, R.B., Shuman, C.A., Anandakrishnan, S., 1995. Dominant control of atmospheric circulation on snow accumulation in central Greenland. Nature 373, 52–54.

Kaufman, D.S., Hopkins, D.M., 1985. Late Cenozoic radiometric dates, Seward and Baldwin Peninsulas and adjacent continental shelf, Alaska. US Geological Survey Open-File Report 85-374.

Kaufman, D.S., Miller, G.H., Stravers, J.A., Andrews, J.T., 1993. Abrupt early Holocene (9.9–9.6 ka) ice-stream advance at the mouth of Hudson Strait, Arctic Canada. Geology 21, 1063–1066.

Kay, P.A., 1979. Multivariate statistical estimates of Holocene vegetation and climate change, forest–tundra transition, NWT, Canada. Quaternary Research 11, 125–140.

Kelly, M., 1980. The status of the neoglacial in western Greenland. Rapport Grønlands Geologiske Undersøgelse 64, 1–26.

Kerwin, M.W., Overpeck, J.T., Webb, R.S., DeVernal, A., Rind, D.H., Healy, R.J., 1999. The role of oceanic forcing in mid-Holocene Northern Hemisphere climatic change. Paleoceanography 14, 200–210.

Kerwin, M.W., Overpeck, J.T., Webb, R.S., Anderson, K.H. submitted. Pollen-based summer temperature reconstructions for the eastern Canadian boreal forest, subarctic, and Arctic. Quaternary Science Reviews, submitted for publications.

Keyser, A.R., Kimball, J.S., Nemani, R.R., Running, S.W., 2000. Simulating the effects of climatic change on the carbon balance of North American high-latitude forests. Global Change Biology 6 (Suppl. 1), 185–195.

Kirby, M.E., Mullins, H.T., Patterson, W.P., Burnett, A.W., 2002. Late glacial–Holocene atmospheric circulation and precipitation in the northeast United States inferred from modern calibrated stable oxygen and carbon isotopes. Bulletin Geological Society of America 114, 1326–1340.

Koç, N., Jansen, E., 1994. Response of the high latitude Northern Hemisphere to orbital climate forcing: evidence from the Nordic Seas. Geology 22, 523–526.

Koç, N., Jansen, E., Haflidason, H., 1993. Paleooceanographic reconstruction of surface ocean conditions in the Greenland, Iceland and Norwegian Seas through the last 14 ka based on diatoms. Quaternary Science Reviews 12, 115–140.

Koerner, R., Fisher, D., 1990. A record of Holocene summer climate from a Canadian high-Arctic ice core. Nature 343, 630–631.

Kozhevnikov, Yu.P., 1981. Ecology-floristic changes in the middle part of the Anadyr River basin. In: Mazurenko, M.T. (Ed.), Biology of Plants and Flora of North of the Far East. Institute of Biological Problems of the North, Far East Branch. USSR Academy of Sciences, Vladivostok, pp. 65–78.

Kutzbach, J.E., Guetter, P.J., 1986. The influence of changing orbital parameters and surface boundary conditions on climate simulations for the past 18,000 years. Journal of the Atmospheric Sciences 43, 1726–1759.

Lacourse, T., Gajewski, K., 2000. Late Quaternary vegetation history of Sulphur Lake, southwest Yukon Territory, Canada. Arctic 53, 27–35.

Lev, D.J., 1987. Balsam poplar (*Populus balsamifera*) in Alaska: ecology and growth response to climate. MS Thesis, University of Washington, Seattle.

Levac, E., deVernal, A., 1997. Postglacial changes of terrestrial and marine environments along the Labrador coast: palynological evidence from cores 91-045-005 and 91-045-006, Cartwright Saddle. Canadian Journal of Earth Sciences 34, 1358–1365.

Levac, E., deVernal, A., Blake, W.J., 2001. Sea-surface conditions in northernmost Baffin Bay during the Holocene: palynological evidence. Journal of Quaternary Science 16, 353–363.

Leverington, D.W., Mann, J.D., Teller, J.T., 2002. Changes in the bathymetry and volume of Glacial Lake Agassiz between 9200 and 7700 ^{14}C yr B.P. Quaternary Research 57, 244–252.

Levy, L.B., Kaufman, D.S., Werner, A., 2003. Holocene glacier fluctuations, Waskey Lake, northeastern Ahklun Mountains, southwestern Alaska. The Holocene, in press.

Licciardi, J.M., Teller, J.T., Clark, P.U., 1999. Freshwater routing by the Laurentide Ice Sheet during the last deglaciation. In: Clark, P.U., Webb, R.S., Keigwin, L.D. (Eds.), Mechanisms of Global Climate Change at Millennial Time Scales. American Geophysical Union, Washington, DC, pp. 177–201.

Lorenz, S., Grieger, B., Helbig, P., Herterich, K., 1996. Investigating the sensitivity of the atmospheric general circulation model ECHAM3 to paleoclimatic boundary conditions. Geol Rundsch 85, 513–524.

Lozhkin, A.V., Anderson, P.M., Brubaker, L.B., Prokhorova, T.P., 1995. The first results of palynological analyses of lacustrine sediments from Chukotka. Doklady Akademii Nauk 342, 540–542.

Lozhkin, A.V., Anderson, P.M., Brubaker, L.B., Kotov, A.N., Kotova, L.N., Prokhorova, T.P., 1998a. The herb pollen zone from sediments of glacial lakes. In: Simakov, K.V. (Ed.), Environmental Changes in Beringia During the Quaternary. North East Interdisciplinary Research Institute, Far East Branch, Russian Academy of Sciences, Magadan, pp. 96–111.

Lozhkin, A.V., Hopkins, D.M., Solomatkina, T.B., Eisner, W.R., Brigham-Grette, J., 1998b. Radiocarbon dates and palynological characteristics of peat from St. Lawrence Island, Alaska. In: Simakov, K.V. (Ed.), Environmental Changes in Beringia During the Quaternary. North East Interdisciplinary Research Institute, Far East Branch, Russian Academy of Sciences, Magadan, pp. 9–27.

Lozhkin, A.V., Anderson, P.M., Vartanyan, S.L., Brown, T.A., Belaya, B.V., Kotov, A.N., 2001. Reconstructions of late Quaternary paleo-environments and modern pollen data from Wrangel Island (northern Chukotka). Quaternary Science Reviews 20, 217–233.

Luterbacher, J., Xoplaki, E., Dietrich, D., Rickli, R., Jacobeit, J., Beck, C., Gyalistras, D., Schmutz, C., Wanner, H., 2002. Reconstruction of sea level pressure fields over the eastern North Atlantic and Europe back to 500. Climate Dynamics 18, 545–561.

Mann, D.H., Crowell, A.L., Hamilton, T.D., Finney, B.P., 1998. Holocene geologic and climatic history around the Gulf of Alaska. Arctic Anthropology 35, 112–131.

Mann, D.H., Peteet, D.M., Reanier, R.E., Kunz, M.L., 2002. Responses of an Arctic landscape to late glacial and early Holocene climatic changes: the importance of moisture. Quaternary Science Reviews 21, 997–1021.

MacDonald, G., 1983. Holocene vegetation history of the upper Natla River area, Northwest Territories, Canada. Arctic and Alpine Research 15, 169–180.

MacDonald, G.M., 1987. Postglacial vegetation history of the Mackenzie River Basin. Quaternary Research 28, 245–262.

MacDonald, G.M., Gajewski, K., 1992. The northern treeline of Canada. In: Janelle, D.G. (Ed.), Geographical Snapshots of North America. Guilford Press, New York, pp. 34–37.

MacDonald, G.M., McLeod, T.K., 1996. The Holocene closing of the 'ice-free' corridor. Quaternary International 32, 87–95.

MacDonald, G.M., Edwards, T., Moser, K., Pienitz, R., 1993. Rapid response of treeline vegetation and lakes to past climate warming. Nature 361, 243–246.

Manley, W.F., 2002. Postglacial flooding of the Bering Land Bridge: a geospatial animation: INSTAAR, University of Colorado, v1, http://instaar.colorado.edu/QGISL/bering_land_bridge.

Mayewski, P.A., Meeker, L.D., Twickler, M.S., Whitlow, S.I., Yang, Q., Lyons, W B., Prentice, M., 1997. Major features and forcing of high-latitude Northern Hemisphere atmospheric circulation using a 110,000-year-long glaciochemical series. Journal of Geophysical Research 102, 26345–26366.

McCulloch, D., Hopkins, D.M., 1966. Evidence for an early recent warm interval in northwestern Alaska. Geological Society of America Bulletin 77, 1089–1108.

McGowan, S., Ryves, D.B., Anderson, N.J., 2003. Holocene records of effective precipitation in west Greenland. The Holocene 13, 239–249.

Miller, G., Mode, W., Wolfe, A., Sauer, P., Bennike, O., Forman, S., Short, S., Stafford Jr., T., 1999. Stratified interglacial lacustrine sediments from Baffin Island, Arctic Canada: chronology and paleoenvironmental implications. Quaternary Science Reviews 18, 789–810.

Mitchell, J.F.B., 1990. Greenhouse warming: is the mid-Holocene a good analogue? Journal of Climate 3, 1177–1192.

Mitchell, J.F.B., Grahame, N.S., Needham, K.J., 1988. Climate simulations for 9000 years before present: seasonal variations and effect of the Laurentide Ice Sheet. Journal of Geophysical Research 93, 8283–8303.

Mock, C.J., Bartlein, P.J., Anderson, P.A., 1998. Atmospheric circulation patterns and spatial climatic variations in Beringia. International Journal of Climatology 18, 1085–1104.

Mode, W., 1980. Quaternary stratigraphy and palynology of the Clyde Foreland, Baffin Island, N.W.T., Canada. Ph.D. Dissertation, University of Colorado, Boulder, 233pp.

Mode, W., Jacobs, J., 1987. Surficial geology and palynology, inner Frobisher Bay. In: Glacial Geology and Holocene events, southern Baffin Island, NWT: Guidebook for Field Trip C2. 12th International Congress, International Union for Quaternary Research, Ottawa, Ont., pp. 53–62.

Moore, J.J., 1996. Late Quaternary glacial and climatic history of the Cape Dyer area eastern Cumberland Peninsula, Baffin Island, Canada: a rock magnetic and varved sediment investigation of Donard Lake. Master's Thesis, University of Colorado, Boulder, 175pp.

Moore, J.J., Hughen, K.A., Miller, G.H., Overpeck, J.T., 2001. Little Ice Age recorded in summer temperature reconstruction from varved sediments of Donard Lake, Baffin Island, Canada. Journal Paleolimnology 25, 503–517.

Moritz, R.E., Bitz, C.M., Steig, E.J., 2002. Dynamics of recent climate change in the Arctic. Science 297, 1497–1502.

Moser, K., MacDonald, G., 1990. Holocene vegetation change at treeline north of Yellowknife, Northwest Territories, Canada. Quaternary Research 34, 227–239.

Mott, R., 1978. *Populus* in late-Pleistocene pollen spectra. Canadian Journal of Botany 56, 1021–1031.

Mysak, L.A., Power, S.B., 1992. Sea-ice anomalies in the western Arctic and Greenland–Iceland Sea and their relation to an interdecadal climate cycle. Climatological Bulletin 26, 147–176.

Nelson, R.E., Carter, L.D., 1987. Paleoenvironmental analysis of insects and extralimital *Populus* from an early Holocene site on the Arctic Slope of Alaska. Arctic and Alpine Research 19, 230–241.

Nesje, A., Johannessen, T., 1992. What were the primary forcing mechanisms of high-frequency Holocene climate and glacier variations? The Holocene 2, 79–84.

Nichols, H., 1975. Palynological and paleoclimatic study of the late Quaternary displacement of the boreal forest–tundra ecotone in Keewatin and Mackenzie, NWT, Canada. University of Colorado, Institute of Arctic and Alpine Research Occasional Paper15, 87pp.

Noren, A.J., Bierman, P.R., Steig, E.J., Lini, A., Southon, J.A., 2002. Millennial-scale storminess variability in the northeastern United States during the Holocene. Nature 419, 821–824.

O'Brien, S.R., Mayewski, P.A., Meeker, L.D., Meese, D.A., Twickler, M.S., Whitlow, S.I., 1995. Complexity of Holocene climate as reconstructed from a Greenland ice core. Science 270, 1962–1964.

Oswald, W., Brubaker, L., Anderson, P., 1999. Late Quaternary vegetational history of the Howard Pass area, northwestern Alaska. Canadian Journal of Botany 77, 570–581.

Payette, S., Lavoie, C., 1994. The Arctic treeline as a record of past and recent climatic changes. Environmental Reviews 2, 78–90.

Peltier, W.R., 1994. Ice age paleotopography. Science 265, 195–201.

Pfeffer, W.T., Dyurgerov, M., Kaplan, M., Dywer, J., Sassolas, C., Jennings, A., Raup, B., Manley, W., 1997. Numerical modeling of late glacial Laurentide advance of ice across Hudson Strait: insights into terrestrial and marine geology, mass balance, and calving flux. Paleoceanography 12, 97–110.

Pienitz, R., Smol, J., MacDonald, G., 1999. Paleolimnological reconstruction of Holocene climatic trends from two boreal treeline lakes, Northwest Territories, Canada. Arctic, Antarctic, and Alpine Research 31, 82–93.

Pienitz, R., Smol, J.P., Last, W.M., Leavitt, P.R., Cumming, B.F., 2000. Multi-proxy Holocene palaeoclimatic record from a saline lake in the Canadian Subarctic. The Holocene 10, 673–686.

Pollard, D., Bergengren, J.C., Stillwell-Soller, L.M., Felzer, B., Thompson, S.L., 1998. Climate simulations for 10000 and 6000 years BP using the GENESIS global climate model. Paleoclimates 2, 183–218.

Porter, L., 1988. Late Pleistocene fauna of Lost Chicken Creek, Alaska. Arctic 41, 303–313.

Rampton, V.N., 1988. Quaternary geology of the Tuktoyaktuk coastlands, Northwest Territories. Geological Survey of Canada, Memoir 423.

Richard, P.J.H., 1977. Histoire post-wisconsinienne de la végétation du Quebec méridional par l'analyse pollinique. Service de la recherche, Direction générale des forêts, Ministère des Terres et Forêts du Québec. Publications et rapports divers. Tome 1, xxiv + 312pp.; tome 2, 142pp.

Richard, P.J.H., 1981. Paléophytogéographie postlaciaire en Ungava par l'analyse pollinique. Paléo-Quebec No. 13, 154pp.

Richard, P.J.H., 1995. Le couvert vegetal du Québec-Labrador il y a 6000 ans BP: Essai. Géographie Physique et Quaternaire 49, 117–140.

Rimbu, N., Lohmann, G., Felis, T., Pätzold, 2001. Arctic Oscillation signature in a Red Sea coral. Geophysical Research Letters 28, 2262–2959.

Rimbu, N., Lohmann, G., Kim, J.-H., Arz, W., Schneider, R., 2003. Arctic/North Atlantic Oscillation signature in Holocene sea surface temperature trends as obtained from alkenone data. Geophysical Research Letters 30 (6), 1280 doi:10.1029/2002GL016570.

Ritchie, J.C., 1984. Past and Present Vegetation of the Far Northwest of Canada. University of Toronto Press, Toronto, 251pp.

Ritchie, J.C., Cwynar, L.C., 1982. The late Quaternary vegetation of the north Yukon. In: Hopkins, D., Matthews Jr., J., Schweger, C., Young, S. (Eds.), Paleoecology of Beringia. Academic Press, New York.

Ritchie, J.C., Hare, F., 1971. Late-Quaternary vegetation and climate near the Arctic tree line of northwestern North America. Quaternary Research 1, 331–342.

Ritchie, J.C., Cwynar, L.C., Spear, R.W., 1983. Evidence from northwest Canada for an early Holocene Milankovitch thermal maximum. Nature 305, 126–128.

Rühland, K., 2001. Diatom assemblage shifts relative to changes in environmental and climatic conditions in circumpolar treeline regions of the Canadian and Siberian Arctic. Ph.D. Dissertation, Queen's University, Kingston, Ont., 265pp.

Rupp, T.S., Chapin III, F.S., Starfield, A.M., 2000. Response of subarctic vegetation to transient climatic change on the Seward Peninsula in northwest Alaska. Global Change Biology 6, 541–555.

Sawada, M., Gajewski, K., deVernal, A., Richard, P., 1999. Comparison of marine and terrestrial Holocene climates in eastern North America. The Holocene 9, 267–278.

Serreze, M.C., Box, J.E., Barry, R.G., Walsh, J.E., 1993. Characteristics of Arctic synoptic activity, 1952–1989. Meteorology and Atmospheric Physics 51, 147–164.

Serreze, M.C., Walsh, J.E., Chapin III, F.S., Osterkamp, T., Dyurgerov, M., Romanovsky, V., Oechel, W.C., Morison, J., Zhang, T., Barry, R.G., 2000. Observation evidence of recent change in the northern high-latitude environment. Climatic Change 46, 159–207.

Shephard, M.E., 1995. Plant ecology and classification of the Yakutat Foreland, Alaska. USDA Forest Service, Alaska Region Report R10-TP-56, Sitka, Alaska, 206pp. + 26pp. of appendices.

Shilo, N.A., Lozhkin, A.V., Anderson, P.M., Belaya, B.V., Stetsenko, T.V., Glushkova, O.Yu., Brigramh-Grette, J., Mellis, M., Minyuk, P.S., Novachek, N., Forman, S., 2001. First continuous pollen record of climate and vegetation changes in the Bering Sea region for the past 300 ka. Doklady Akademii Nauk 376, 231–234.

Shindell, D.T., Schmidt, G.A., Mann, M.E., Rind, D., Waple, A., 2001. Solar forcing of regional climate change during the Maunder Minimum. Science 294, 2149–2152.

Short, S.K., Nichols, H., 1977. Holocene pollen diagrams from subarctic Labrador–Ungava: Vegetational history and climatic change. Arctic and Alpine Research 9, 265–290.

Short, S.K., Andrews, J.T., Williams, K.M., Weiner, N.J., Elias, S.A., 1994. Late Quaternary marine and terrestrial environments, northwestern Baffin Island, Northwest Territories. Géographie Physique et Quaternaire 48, 85–95.

Smith, L.M., 2001. Holocene environmental reconstruction of the continental shelves adjacent to the Denmark Strait. Ph.D. Dissertation, University of Colorado, Boulder, 219pp.

Smith, R.I., 2002. Diatom-based Holocene paleoenvironmental records from continental sites on northeastern Ellesmere Island, high Arctic, Canada. Journal of Paleolimnology 27, 9–28.

Smith, L.M., Miller, G.H., Otto-Bliesner, B., Shin, S-I., 2003. Sensitivity of the Northern Hemisphere climate system to extreme changes in Holocene Arctic sea ice. Quaternary Science Reviews 22, 645–658.

Smol, J.P., 1983. Paleophycology of a high Arctic lake near Cape Herschel, Ellesmere Island. Canadian Journal of Botany 61, 2195–2204.

Sorenson, C.J., 1977. Reconstructed Holocene bioclimates. Annals of the Association of American Geographers 67, 214–222.

Spear, R.W., 1983. Paleoecological approaches to a study of treeline fluctuations in the Mackenzie Delta Region, Northwest Territories. Preliminary results. In: Morisset, P., Payette, S. (Eds.), Tree-Line Ecology. Nordicana 47, 61–72.

Spear, R.W., 1993. The palynological record of Late-Quaternary Arctic tree-line in northwestern Canada. Review of Palaeobotany and Palynology 79, 99–111.

Steig, E.J., 1999. Mid-Holocene climate change. Science 286, 1485–1487.

Stuiver, M., Reiner, P.J., 1993. Extended ^{14}C data base and revised CALIB 3.0 ^{14}C age calibration program. Radiocarbon 35, 215–230.

Stuiver, M., Grootes, P.M., Braziunas, T.F., 1995. The GISP2 δ^{18}O climate record of the past 16,500 years and the role of the Sun, ocean, and volcanoes. Quaternary Research 44, 341–354.

Szeicz, J.M., MacDonald, G.M., 2001. Montane climate and vegetation dynamics in easternmost Beringia during the Late Quaternary. Quaternary Science Reviews 20, 247–257.

Szeicz, J.M., MacDonald, G.M., Duk-Rodkin, A., 1995. Late Quaternary vegetation history of the central Mackenzie Mountains, Northwest Territories, Canada. Palaeogeography, Palaeoclimatology, Palaeoecology 113, 351–371.

Teller, J.T., Leverington, D.W., Mann, J.D., 2002. Freshwater outbursts to the oceans from glacial Lake Aggassiz and their role in climate change during the last deglaciation. Quaternary Science Reviews 21, 879–888.

TEMPO, 1996. Feedbacks between climate and the boreal forest during the Holocene epoch. Global Biogeochemical Cycles 10, 727–736.

TenBrink, N.W., Waythomas, C., 1985. Late Wisconsin glacial chronology of the north-central Alaska Range; a regional synthesis and its implications for early human settlements. In: Powers, W.R. (Ed.), North Alaska Range Early Man Project. National Geographic Society, Washington, DC, pp. 15–32.

Thompson, D.W.J., Wallace, J.M., 1998. The Arctic Oscillation signature in the wintertime geopotential height and temperature fields. Geophysical Research Letters 25, 1297–1300.

Vardy, S.R., Warner, B.G., Aravena, R., 1997. Holocene climate effects on the development of a peatland on the Tuktoyaktuk Peninsula, Northwest Territories. Quaternary Research 47, 90–104.

Vardy, S.R., Warner, B.G., Aravena, R., 1998. Holocene climate and the development of a subarctic peatland near Inuvik, Northwest Territories, Canada. Climatic Change 40, 285–313.

Vartanyan, S.L., 1997. The last Beringian survivors: Interdisciplinary paleogeographical studies on Wrangel Island, east Siberia.

Beringian Paleoenvironments Workshop, Florissant, CO, pp. 155–158.

Vasari, Y., Vasari, A., 1990. L´histoire Holocéne des lacs Islandais. In: Devers, S. (Ed.), Pour Jean Malaurie. Editions Plon, Paris, pp. 277–293.

Vavrus, S.J., 1999. The response of the coupled Arctic sea ice–atmospheric system to orbital forcing and ice motion at 6 kyr and 115 kyr BP. Journal of Climate 12, 873–896.

Vavrus, S.J., Harrison, S.P., in press. The impact of sea ice dynamics on the Arctic climate system. Climate Dynamics.

Viau, A., 2003. Millennial-scale climate variability in North America during the past 14,000 years. Ph.D. dissertation, University of Ottawa, Ontario, 319pp.

Wagner, B., Melles, M., 2001. A Holocene seabird record from Raffles Sø sediments, East Greenland, in response to climatic and oceanic changes. Boreas 30, 228–239.

Wagner, B., Melles, M., 2002. Holocene environmental history of western Ymer Ø, East Greenland, inferred from lake sediments. Quaternary International 89, 165–176.

Wagner, B., Melles, M., Hahne, J., Niessen, F., Hubberten, H.W., 2000. Holocene climate history of Geographical Society Ø, east Greenland-evidence from lake sediments. Palaeogeography, Palaeoclimatology, Palaeoecology 160, 45–68.

Wastl, M., Stötter, J., Caseldine, C., 2001. Reconstruction of Holocene variations of the upper limit of tree or shrub birch growth in northern Iceland based on evidence from Vesturárdalur-Skíadalur, Tröllaskagi. Arctic, Antarctic, and Alpine Research 33, 191–203.

Weber, F.R., Hamilton, T.D., Hopkins, D.M., Repenning, C.A., Haas, H., 1981. Canyon Creek: a late Pleistocene vertebrate locality in interior Alaska. Quaternary Research 16, 167–180.

White, J.W.C., Barlow, L.K., Fisher, D., Grootes, P., Jouzel, J., Johnsen, S.J., Stuiver, M., Clausen, H., 1997. The climate signal in the stable isotopes of snow from summit, Greenland: results of comparisons with modern climate observations. Journal of Geophysical Research 102 (C12), 26425–26439.

Willemse, N., Törnqvist, T., 1999. Holocene century-scale temperature variability from West Greenland lake records. Geology 27, 580–584.

Wolfe, A., 1994. Late Wisconsinan and Holocene diatom stratigraphy from Amarok Lake, Baffin Island, NWT, Canada. Journal of Paleolimnology 10, 129–139.

Wolfe, A., 1996. A high-resolution late-glacial and early Holocene diatom record from Baffin Island, eastern Canadian Arctic. Canadian Journal of Earth Sciences 33, 928–937.

Wolfe, B.B., Edwards, T.W.D., Aravena, R., MacDonald, G.M., 1996. Rapid Holocene hydrologic change along boreal treeline revealed by δ^{13}C and δ^{18}O in organic lake sediments, Northwest Territories, Canada. Journal of Paleolimnology 15, 171–181.

Wolfe, B.B., Edwards, T.W.D., Aravena, R., Forman, S.L., Warner, B.G., Velichko, A.A., MacDonald, G.M., 2000. Holocene paleohydrology and paleoclimate at treeline, north-central Russia, inferred from oxygen isotope records in lake sediment cellulose. Quaternary Research 53, 319–329.

Wooller, M.J., Francis, D., Fogel, M.L., Miller, G.H., Walker, I.R., Wolfe, A.P, in review. Quantitative paleotemperature estimates from δ^{18}O in chironomid head capsules from Arctic lake sediment. Geology.

Zielinski, G.A., Mayewski, P.A., Meeker, L.D., Whitlow, S., Twickler, M.S., Morrison, M., Meese, D.A., Gow, A.J., Alley, R.B., 1994. Record of volcanism since 7000 B.C. from the GISP2 Greenland ice core and implications for the volcano-climate system. Science 264, 948–952.

Zoltai, S.C., 1995. Permafrost distribution in peatlands of west-central Canada during the Holocene warm period 6000 years B.P. Géographie Physique et Quaternaire 49, 45–54.

Zoltai, S.C., Tarnocai, C., 1975. Perennially frozen peatlands in the western Arctic and Subarctic of Canada. Canadian Journal of Earth Sciences 12, 28–43.

Zoltai, S.C., Vitt, D.H., 1990. Holocene climatic change and the distribution of peatlands in western interior Canada. Quaternary Research 33, 231–240.